Title: Retinal damage induced by commercial light emitting diodes (LEDs).

Authors: Jaadane I, Boulenguez P, Chahory S, Carré S, Savoldelli M, Jonet L, Behar-Cohen F, Martinsons C, Torriglia A

Journal: Free radical biology & medicine

Year: 2015 Jul

Volume: 84

Pages: 373-84

DOI: 10.1016/j.freeradbiomed.2015.03.034

Retinal damage induced by commercial Light Emitting Diodes (LED)

Imene Jaadane[1], Pierre Boulenguez[2], Sabine Chahory[3], Samuel Carré[2], Michèle Savoldelli[1], Laurent Jonet[1], Francine Behar-Cohen[1,4], Christophe Martinsons[2], Alicia Torriglia[1].

1. INSERM U1138. Centre de Recherches des Cordeliers. Université Paris Descartes, Université Pierre et Marie Curie. Paris. France

2. CSTB, Centre Scientifique et Technique du Bâtiment. Division Eclairage et électromagnétisme. Saint Martin d'Heres. France

3. ENVA, Ecole Nationale Vétérinaire d'Alfort. Maison Alfort. France

4. Hôpital Ophtalmique Jules Gonin. Lausanne. Switzerland.

Corresponding author: Alicia TORRIGLIA, INSERM U1138. Centre de Recherches des Cordeliers, 15, rue de l'école de Médecine, 75006. Paris. France.

E-mail: alicia.torriglia@inserm.fr

Keywords: LED, retinal degeneration, apoptosis, necrosis, necroptosis, stress response, oxidative stress, blue light, wavelength.

Highlights:

LED light induces oxidative stress and retinal injury.
LED light induces photoreceptors death by necrosis and apoptosis.

The blue component of LED is the major cause of retinal damage.

Abstract

Background: Spectra of "white LED" are characterized by an intense emission in the blue region of the visible spectrum, absent in day light spectra. This blue component and the high intensity of emission are the main sources of concern about the health risks of LEDs with respect to their toxicity to the eye and the retina.

Objective: The aim of our study was to elucidate the role of blue light from LEDs in retinal damage.

Methods: Commercially available white LED and four different blue LEDs (507, 473, 467 and 449 nm) were used for exposure experiments on Wistar rats. Immunohistochemical stain, transmission electron microscopy and western blot were used to exam the retinas. We evaluated LED-induced retinal cell damage by studying oxidative stress, stress response pathways and the identification of cell death pathways.

Results: LED light caused a state of suffering of the retina with oxidative damage and retinal injury. We observed a loss of photoreceptors and the activation of caspase independent apoptosis, necroptosis and necrosis. A wavelength dependence of the effects was observed.

Conclusion: Phototoxicity of LEDs on the retina is characterized by a strong damage of photoreceptors and by the induction of necrosis.

INTRODUCTION

Retinal degenerations, whether genetic or not, involve death of photoreceptors. Environmental factors such as smoking, obesity and hypertension are important in the progression of the different retinopathies [1]. In addition, the exposure to intense natural or artificial light can be detrimental to eye tissues by causing photochemical damages. Many studies have been conducted to evaluate the effect of light on the evolution of pre-existing retinopathy [2]. For the last few years this interest has been concentrated on age related macular degeneration (AMD), a leading pathology of the elderly in western countries [3]. After many conflicting studies it was concluded that light is a risk factor in the early stages of AMD although it is not recognized as an aggravating factor for the pathology [4-6].

The retinal damages induced by light depend on radiation intensity, radiation wavelength and time of exposure [7-8]. Light-induced retinal lesions are characterized by a degeneration of photoreceptors outer segments leading to their death by apoptosis [9-10].

Recently, the use of new technologies in domestic lighting induced a renewal of the interest on the effects of light on the retina. Among these new devices, Light emitting diodes (LEDs) are at the center of this interest. From a technical point of view LEDs have many advantages such as low energy consumption, high mechanical strength and, especially, long life. One of the major concerns with the use of this technology is the emission spectrum of LEDs. The spectrum of LEDs is characterized by an intense blue light component absent in the day light spectra [11]. In recent years, governmental agencies such as the ANSES (French Agency for Food, Environmental and Occupational Health and Safety) in 2010 stressed the need for extensive experimental studies on the phototoxicity of LEDs to confirm or refute the fears raised by researchers, ophthalmologists and physicists concerning the intensive use of these devices. Actually, the most commonly used LEDs present a high luminance level and generate a visual discomfort related to the "punctual" character of the emitting surfaces. In addition, the spectral imbalance of white LEDs available on the market, due to the production of white light by the processing of a high-frequency radiation and re-emission in a complementary wavelength, exposes the eye to residual short wavelengths radiations, the most dangerous to the retina. This problem could be increased by a reduction of the pupillary contraction, stimulated at around 480 nm, a region of low emission in the spectrum of some LEDs, resulting in an increase of retinal light exposure.

In this study, we investigate, in rats, the molecular mechanism of retinal degeneration by using five different LEDs: white LED, green LED (507 nm) and three blue LEDs (449, 467, 473 nm) to evaluate the role of blue radiation in cellular damage and the progression of retinal lesions.

MATERIALS AND METHODS

Animals

Six-week-old male Wistar rats were purchased from Janvier labs and kept one week for adaptation in our animal facilities in a light cycle of 12 h. All procedures were in compliance with the animal use and care committee of the National Veterinary School of Alfort.

Light source

We used two types of lighting devices built and characterized by the Lighting and electromagnetism division of the Scientific and Technical Center for Building (CSTB, Saint Martin d'Heres, France): the first contains only white LEDs (Xanlite XXX Evolution 5W). The second device has four types of LEDs with different wavelengths in the blue region of the spectrum: green LED (507 nm) and three blue LEDs (449, 467, 473 nm) (Table 1). Both devices possess a diffuser improving the directional uniformity of the radiation. The spectral distributions and intensities of light sources were established and tested by the CSTB. The spectra of emission of the different devices are shown on supplementary figure 1. The construction of the blue device is seen in supplementary figure 2. Dose of exposure was calculated by using dedicated software developed by the CSTB for these sets of experiments. The calculations relied on in situ spectrophotometric measurements and on a model of the Wistar rat vision and behavior. For each type of source, spectral irradiance and uniformity were measured using a fiber optic spectrophotometer with a diffusing head (Ocean Optics-R2000+). In the lighting device only the ceiling of the cage was emitting light. Thus, at a given instant, retinal dose of a freely moving rat depended upon his head posture. For the overall dose estimation, it was estimated that, on average, a rat keeps his head aligned with his body. Following the arguments given in the review article [12], the eye of a rat was modeled as an hemisphere. All the formalism used is described in supplementary information 1.

Light exposure

Wistar rats were kept in transparent cages placed under the light sources suspended 25 cm above the top of cages. The rats were exposed to a constant light for 6, 12, 18, 24, 48 and 72 h, without been previously dark-adapted. After illumination, the rats were sacrificed using Sodium pentobarbital (Ceva, La Ballastiere, France) at lethal dose by intraperitoneal injection. Their eyes were immediately enucleated and fresh-frozen in optical cutting temperature (OCT) compound (Tissue Tek compound Sakura) using liquid nitrogen and stored at -80 °C until sectioning. 10µm cryosections were prepared by using a cryostat (Leica CM 3050S) and stored at -20°C until immunohistochemical analysis. Alternatively, for biochemical experiments, neuroretina was dissected and frozen immediately at -20 C.

Dilated Fundus Examination

After the exposure rats were examined by Dr. S. Chahory (ophthalmological veterinary) using a 28D lens (Heine Optotechnik Herrsching, Germany).

Intravitreal injection of propidium iodide (PI)

After light exposure, the rats were anesthetized by an intra peritoneal injection of Sodium Pentobarbital at 25 mg/kg. A local anesthesia was performed by an instillation of Tetracaine 1% (Faure, Novartis Pharma). The intravitreal injection of propidium iodide (Sigma Aldrich, Saint-Quentin Fallavier, France) was carried out under a surgical microscope using a 30G needle mounted on an insulin syringe (BD Micro-Fine, Becton Dickinson S.A., Le Pont de Claix, France). Propidium iodide was injected at a concentration of 1 µg per eye in a volume of 10 µL of Balanced Salt Solution (BSS, Bausch and Lomb). The rats were sacrificed using sodium pentobarbital (Ceva, La Ballastiere, France) at lethal dose by intraperitoneal injection. Their eyes were immediately enucleated after killing and fixed in 4% paraformaldehyde for 2 h at room temperature, washed several times with PBS and then embedded in optimal cutting-temperature (OCT) for preparation of cryosections.

Protein extraction from light exposed retinas

After defrosting, the retinas were homogenized in 20% weight–volume of M-PER extraction reagent (Thermo Scientific, Illkirch, France), using a pellet pestle motor homogenizer (Kontes) on an ice bed. The homogenate was then incubated on ice for 15 min and centrifuged (15,000 g, 4°C) for 15 min. Supernatant was recovered for Western Blot analysis.

Western Blot

After extraction of retinal proteins, their amount was measured with the bicinchoninic acid (BCA)^{TM} Protein Assay Kit (Thermo Scientific, Illkirch, France), according to the manufacturer's instructions. Bovine serum albumin (BSA) was used as standard. Laemmli sample buffer was added for Western Blot analysis**.** Extracted proteins were separated in a 12% SDS-PAGE, immobilized on nitrocellulose membrane (Protan ®, Whatman ®, GE Healthcare, Versailles, France) and blotted with specific primary antibody at 1/1000 dilution: anti-PKC zeta (Santa Cruz sc-216, Clinisciences, Nanterre, France), anti-phospho-PKC zeta (Santa Cruz sc-12894R, Clinisciences, Nanterre, France), anti-Actin (Santa Cruz sc-1616, Clinisciences, Nanterre, France), anti-LEI/L-DNase II (produced in our laboratory) [13]. The secondary antibodies conjugated to HRP (Vector, Eurobio, Les Ulis, France) were used in a 1/5000 dilution. Finally, Luminata Forte Western HRP Substrate (Millipore, Merck Chimie, Fontenay sous Bois, France) was used to reveal the signal.

Poly-ADP-ribose polymerase (PARP-1) immunoblot

After enucleating the eyes the retina were extracted, rinsed in PBS and homogenized in Laemmli sample buffer using a pellet pestle motor (Kontes). Proteins were measured as before. 40 µg of protein were loaded on the top of a 10% SDS-PAGE, and transferred to a High-Bound ECL nitrocellulose membrane (Protan, Whatman, GE Healthcare, Versailles, France). PARP-1 was developed using the monoclonal C-2-10 antibody (Biovision, Milpitas, USA) diluted in PBS Tween 0.1% at 1/500 dilution. Development of the labeled bands was done by using a HRP-conjugated secondary antibody and the Luminata Forte Western HRP Substrate (Millipore, Eurobio, Les Ulis, France).

Immunohistochemistry

Cryosections of the eyes were washed twice with PBS containing Ca^{2+} and Mg^{2+}, fixed in 4% paraformaldehyde for 15 min at room temperature (all steps were performed at room temperature) and then washed twice with PBS. Permeabilization was performed with 0.3% Triton X-100 for 20min. Then, the cryosections were washed twice with PBS, non-specific protein binding sites were blocked by 1 h incubation in a blocking buffer containing 1% non-fat milk in PBS. Samples were then incubated with specific primary antibodies in 0.1% non-fat milk in PBS diluted at 1/100 for 1 h. A complete list of the antibodies used is shown on Table 2. This was followed by two washes with PBS and incubation for 1 h with a 1/500 dilution of specific secondary antibodies (Invitrogen, Life Technologies, Saint Aubin, France). Samples were washed twice with PBS, incubated for 5 min with 4,6 di-aminidino-2-phenyl indoledichloride DAPI 1/5000, (Sigma Aldrich, Saint-Quentin Fallavier, France) and then washed again three times with PBS. Finally, cryosections were coverslipped with fluoromount (Sigma, Saint-Quentin Fallavier, France). Immunoreactivity was visualised using fluorescence microscopy with an Olympus microscope BX51 (Olympus France, Rungis, France) or a Zeiss LSM 710 confocal microscope.

Terminal transferase dUTP nick end labeling (TUNEL)

Cryosections were air dried and fixed in 4% paraformaldehyde 15 min at room temperature and washed twice with PBS. After permeabilization with 0.3% Triton X-100 in PBS for 20 min at room temperature and an additional PBS wash, the TUNEL assay was performed using two different protocols. For the classical protocol, cryosections were incubated with the TUNEL reaction Mix (Roche Molecular Biochemical's, Meylan, France) according to the manufacturer's instructions. For the second protocol, the sections were previously incubated for 30 min with calf intestinal alkaline phosphatase 6.66 U/section (Invitrogen, Life Technologies, Saint Aubin, France) at 37 °C. In both cases, the tissues were rinsed three times after TUNEL reaction with PBS and incubated with DAPI 1/5000. Finally, after three washes with PBS, cryosections were coverslipped with fluoromount (Sigma Aldrich, Saint-Quentin Fallavier, France). Immunoreactivity was visualised using a fluorescence microscopy Olympus microscope BX51 (Olympus France, Rungis, France) or a Zeiss LSM 710 confocal microscope.

Transmission electron microscopy analysis (TEM)

TEM was performed on non-exposed retinas and on retinas exposed 18 h to the white LED. After enucleation the eyes were fixed in 4% glutaraldehyde cacodylate buffer (0.1 M, pH 7.4) for 5 h. Specimens were additionally fixed in 1% osmium tetroxide in cacodylate buffer (0.2 M, pH 7.4) and progressively dehydrated in graduated ethanol solution (50, 70, 95, and 100%) then in propylene oxide. Each area of interest was separated in four samples, included in epoxy resin and oriented. Semi-thin sections (500 nm) were obtained with an ultra microtome (LEICA Ultracut UCT Austria) and stained with toluidine blue. Ultra-thin sections (60 nm) were contrasted by uranyl acetate and lead citrate and analysed with a transmission electron microscope (Philips CM10 Netherlands) with a GATAN ES100W camera (USA).

Results

Dilated fundus examination (DFE) showed no bleaching of the retina.

DFE is a diagnostic procedure used to evaluate the internal ocular health. Until today, regulations of light toxicity on the retina have established ELV (exposure limit values) [14]. These ELV are based on a study of fundus examination following a single exposure to light during 8 h. They establish that light is toxic to the eye when there is a bleaching of the retina. In our study, DFE was done just after exposure by a veterinary ophthalmologist and two assistants. No bleaching of the retina was detected in rats exposed for 12 h to 3 days with the different types of LED used in this study. However, an important chemosis, indicating an edema of the ocular tissues, was present in almost all the animals during the first 24 h of exposure (supplementary figure 3), disappearing thereafter.

The damages and signs of oxidative stress induced by LEDs.

In order to explore the photochemical lesions in the retina, we study inflammation signs that may be associated with chemosis and edema induced by white LED exposure. Semi-thin sections of retina showed an important interphotoreceptor edema (supplementary Figure 4). Immunohistochemistry (IHC) staining of CD11b (integrin αM) and Ionized calcium binding adaptor molecule 1 (Iba 1) on retina exposed for one and two days, showed an activation of microglia and macrophage infiltration in the retina revealing retinal inflammation (Figure 1).

Signs of oxidative stress on DNA/RNA were investigated by 8-hydroxyguanosine (HGN) staining (Figure 2 and supplementary figure 5). Protein oxidation was assessed by nitro-tyrosine (N-Tyr) staining (Figure 2, N-Tyr and supplementary figure 5). The LED exposed rats presented an increase of HGN immunostaining mostly in the inner nuclear layer (INL) and in ganglion cell layer of retina exposed for 18 h (125 J/cm^2), although a faint increase in the labeling of the outer nuclear layer (ONL) was also seen. For the same exposure time, N-Tyr immunostaining was higher in all the retina layers compared to rats kept in normal cycling light (NE) (Figure 2 and supplementary figure 5). However, we found a striking increase in photoreceptor outer segments (POS) and in photoreceptors inner segments (PIS). Moreover, a closer examination of the ONL showed a radial labeling that was prolonged in

some cases to the inner plexiform layer (IPL) and the inner nuclear layer (INL) suggesting a labeling (partial and non exclusive) of the Müller cells. These results revealed that light emitted from commercially available LED induced oxidative damage in the entire retina, at the DNA and protein levels. This damage triggered classical stress responses by increasing the expression of p62 (also called sequestosome) in all the nuclear layers of the retina (Figure 2 p62). As expected a stress reaction was also seen at the Müller cell level characterized by an increase of the intermediate filament glial fibrillary acid protein (GFAP) (Figure 2). Interestingly, this response of the Müller cells was quite early, since we saw it after 12 h of exposure (supplementary figure 5, dose: 81 J/cm²). GFAP, a marker of Müller cells activation [15] was restricted, in normal retina, to the feet of the Muller cells. After 12 h of white LED exposure, increased GFAP immunostaining was detected in the inner limiting membrane. At 18 h (125 J/cm²), some processes of Müller cells extended from outer plexiform layer (OPL) to ganglion cell layer (GCL). Increased GFAP staining was prominent over the entire retina after 24 h (151 J/cm²) of exposure to white LED. These results suggested a reactive gliosis spanning the entire retina following Müller cells activation.

LED-induced retinal degeneration.

To investigate whether LED light induced retinal cell death, DAPI staining was used to reveal morphological changes in the nuclei of cells from retina exposed to LEDs compared to unexposed retina (supplementary figure 6). We observed disorganization and a reduced thickness of the ONL. The decrease in ONL thickness was dependent on the time of exposure and it was maximal at 3 days (453 J/cm²). Note that GNL and INL seemed preserved.

LED-induced retinal cell death.

The decrease in ONL thickness indicated retinal degeneration and suggested the presence of cellular demise. In order to investigate this issue TUNEL assay was used. As seen on figure 3, panel A, many apoptotic cells were detected after 18 h of exposure to white LEDs, but apoptotic cells were also detected thereafter (supplementary figure 7), with a maximum at 48 h of exposure (303 J/cm²).

To study classical apoptosis implication in photoreceptor cell death, we investigated the activation of caspase 3. To do this we used an antibody directed against activated caspase 3 (Figure 3, panel A). On the contrary of what was expected, we did not observe a massive increase in active caspase 3 immunostaining, suggesting that this apoptotic pathway was not involved in cell death. This result drove our attention to the activation of caspase-independent pathways. We investigated first the activation of apoptosis inducing factor (AIF) (Figure 3, panel A). This pathway is activated by the release of AIF from the mitochondria to the nucleus, where it triggers chromatin condensation [16]. Immunohistochemistry analysis of LED exposed retinas showed an increase of AIF staining in ONL and also in INL (Figure 3 panel A and supplementary figure 8). However, although the nuclear layers of the retina were more stained than the control, it was not clear, due to the small amount of cytoplasm in photoreceptors if the staining was really nuclear. To solve this point we counterstained our slides with an antibody against lamin B, a protein of the nuclear envelop and we analyzed the section by confocal microscopy. As seen on figure 3B, upper panel, in light exposed retinas AIF is located inside the nuclei where it forms small aggregates, suggesting the activation of this pathway.

We have previously shown that in light induced retinal degeneration (LIRD) using white fluorescent bulbs, caspases were not activated [17]. Instead, a caspase-independent cell death pathway, the LEI/L-DNase II was involved in photoreceptor degeneration [18]. The activation of this pathway involves the cleavage, by specific proteases, of the cytoplasmic Leukocyte Elastase Inhibitor (LEI), and its transformation into L-DNase II, a nuclear protein [19]. The nuclear translocation of this molecule was investigated as seen on figure 3, panel A (and supplementary figure 8). The same than for AIF, the staining of the nuclear layers of the retina was increased but the nuclear translocation was not clear. As for AIF we examined the sections after lamin B staining. Here again (Figure 3 B, lower panel) after white LED exposure L-DNase II was nuclearized but it was kept at the periphery of the condensed chromatin of the photoreceptor.

The high number of cells labeled by the TUNEL assay and the mild activation of caspase dependent and caspase independent effectors of cell death, lead us to investigate other mechanism that could be involved in photoreceptor demise, particularly those forms of cell death that could give TUNEL positive labeling. We analyzed then the activation of programmed necrosis. This form of cell death is promoted and controlled by RIP kinases (receptor-interacting protein) a family of proteins that has been demonstrated to control and to

promote necrosis [20]. We showed that RIP 1 and RIP 3 were increased in continuous light exposure conditions (Figure 3, panel A) suggesting an activation of necrosis. To verify this we analyzed the degradation pattern of poly-ADP-Ribose polymerase 1 (PARP-1) (Figure 3 panel C). During apoptosis, cleavage of PARP-1 by caspases 3 and 7 produced two fragments of 89 and 24 kDa [21]. During necrosis, however, a fragment of 62 kDa is produced [22-23]. A fragment of 44 kDa has also been described as the product of PARP-1 cleavage by calpain or cathepsin D [24]. In our experiments, after exposure to white LEDs (18 h, 125 J/cm^2), the 62 kDa fragment was clearly seen, as well as the fragment of 44 kDa. Moreover, a clear increase of the PARP-1 expression was seen in light exposed retinas. This was concomitant to an increase of auto-ADP ribosylated PARP-1 (Figure 3C, 250 kDa band). Taken together these data were in accord with the activation of necrosis.

In order to further document the activation of necrosis, histological and transmission electron microscopy (TEM) was performed to validate these findings and to explore morphological abnormalities of photoreceptors. Histological examination of semi-thin retinal sections showed that retina exposed to white LED for 18 h (125 J/cm^2) developed prominent interstitial spaces between photoreceptors nuclei and across the ONL (supplementary figure 4). TEM showed different alteration of photoreceptors according to the explored area (Figure 4). At the POS (photoreceptor outer segment) level a complete disorganization of the ordered structure was seen after LED exposure. At the nuclei level several alterations were recorded. The dilation of the interphotoreceptor space was increased (white arrow head), typical condensed nuclei, reminding apoptotic nuclei were seen (black arrow), as well as dilated nuclei reminding necrotic cells (white arrows). Alterations were also found at the PIS (photoreceptor inner segments): edema of the PIS, alteration of mitochondria (arrow head) and edema of the endoplasmic reticulum (arrow). These are typical characteristics of necrotic cells.

The involvement of blue radiation in LED-induced damages.

As seen on supplementary figure 1, upper panel, the white LED used for the described experiments have an important emission in the blue region of the spectrum. In order to evaluate the effect of this blue light we conducted a new set of experiments where rats were exposed to blue LEDs. Four commercially available LEDs were used: the blue LED and the

blue-green LED from Nichia corporation (that we will call hereafter Nichia blue and Nichia blue-green respectively), and the blue LED and the Royal blue LED from Cree industries (called hereafter Cree Blue and Cree Royal Blue). The four LEDs were mounted by group of four in the device described on supplementary figure 2, designed and built for the intended experiments.

For blue LEDs almost the same parameters as for white LEDs were evaluated, however, the lesions found were more important so that we limited the exposure to 24 h. Figure 5 shows representative results of oxidative stress induction obtained after 18 h of exposure to the different LED. The increase of HGN labeling was comparable to the one obtained after white LED exposure although the dose of exposure were quite different. However, Cree Royal Blue LED seemed to increase this marker of oxidative stress, mostly in the INL. Concerning N-Tyr, only the Cree Royal blue LED produced the same degree of modification of the proteins at the RIS and ROS level than white LED. As immunofluorescence is not a quantitative assay we investigate the difference in N-Tyr levels by western blot (Figure 5B). As it is seen in Figure 5, blue diodes (but not Nichia blue green) increased the nitric oxidation of tyrosines. The Cree Royal Blue presented the higher amount of nitrosylated proteins. Concerning the stress response, as with white LED, we also found an increase of p62. In order to compare the different diodes between them we evaluated p62 by western blot after 18 h of exposure (Figure 6 A). We saw a global increase of p62 but, as it can be seen on figure 6, panel A, the rate of cleavage of p62 is increased in Cree LEDs (CRB and CB). This cleavage is thought to disrupt the protective processes of autophagy and NFkB activation [25], we investigated then the activation of both NFkB and PKC zeta (Figure 6, panels B and C, and supplementary Figure 9). PKC zeta is an upstream activator of NFkB that we have already seen as activated in LIRD (unpublished results). The activation of PKC zeta, as materialized by its phosphorylated form, seemed activated in all but Nichia Blue Green LEDs. This is also the case for phospho-NFkB, suggesting that the stress induced by pure blue LEDs was different from the stress induced by an almost green device. It is interesting to note that the PKC zeta pattern was completely different when rats were exposed to Nichia Blue Green radiation. This was the only situation in which a cleavage of the enzyme was seen (Figure 6 panel B).

Taken together these results indicated that the blue-rich light induced a more profound cellular stress, mainly affecting photoreceptors. This cellular stress induced a proportional cellular response.

We next investigated the toxicity of the blue LEDs by examining cell death, as before. TUNEL labeling indicated the presence of dying photoreceptors in all situations (Figure 7). Interestingly, when we looked for caspase 3 activation, cleaved caspase 3 labeling was only found in INL after blue LED exposure. This was different from white LEDs, where no activation of caspase 3 was found (Figure 3). Moreover, it was surprising to see such an important activation of caspase 3 without a single TUNEL positive cell in the INL layer.

Following the same scheme than for white LEDs, we evaluated the caspase independent pathways. This was done after 18 h of exposure. Results are seen on figure 8. AIF seemed activated only in Nichia Blue Green LEDs, as indicated by the presence of truncated AIF (Figure 8 A, upper panel, arrow head). L-DNase II is also activated (Figure 8 A, middle panel) but in a different way, as seen in figure 8 A, lower panel; that shows the quantification of the ratio L-DNase II/LEI. L-DNase II is activated in blue-rich LEDs (CRB, CB and NB), and this activation is the most important in Cree Royal blue LED.

In order to evaluate the presence of necrosis we studied RIP 1 and RIP 3 after 18 h of exposure. RIP 1 was cleaved when using Cree devices, indicating the presence of necrosis, while RIP 3 was clearly cleaved when rats were exposed to Nichia Blue Green light. As this fragment is usually produced by caspase 8 we looked for the activation of this enzyme. The lower panel of figure 8 B shows a representative experiment of this study in which the upper band represents the procaspase 8, while the lower band (arrow head) represents the active caspase 8. Taken together these results indicate the activation by blue light of caspase independent pathways, but mostly the activation of necrosis.

The activation of this form of cell death being rare in light-induced retinal degeneration we tried to prove that necrosis was really taking place in the retinas of exposed rats. To do that we used the property of propidium iodide (PI) to label the nuclei of a cell that has lost the integrity of its membrane. To label photoreceptors we injected intravitreally a PI solution after LED exposure, some minutes before sacrifice. The eyes were then enucleated and immediately fixed, mounted, cryosectioned and observed with a fluorescence microscope without any other type of treatment or staining. Figure 8 C shows a representative result of these experiments. Exposed retinas show a very high number of labeled cells situated in the inner part of the ONL. The combination of this technique with a TUNEL staining (Figure 8 C lower panel) clearly shows the presence of TUNEL positive, PI negative cells. These were

apoptotic cells, and PI positive cells that were necrotic cells whether they were or not TUNEL positive.

These data confirmed the degeneration induced by LED light on the retina, indicating a structural loss of photoreceptors and the activation of two cell death pathways: apoptosis and necrosis.

The western blot analysis of white LED exposed retinas (18 h , 125 J/cm^2) show patterns of the above studied molecular markers corresponding to Nichia Blue Green and Nichia Blue LEDs, indicating that these forms of cell demise are also activated by the white LEDs (Figure 8D).

Discussion

In this paper we analyzed the effects of so called "white LEDs" and blue-enriched LEDs on the retina. We show an important damage of the photoreceptors layer after 18 h of exposure. More importantly, the analysis, at the molecular level, of the effectors of cell death shows an activation of necrotic cell death, a rare event in this type of degeneration.

The current regulation [26] establishes that light is toxic to the eye when there is a bleaching of the retina as seen by fundoscopy. In our macroscopic analysis the eyes of rats exposed to LED light show no bleaching, but an important chemosis. This indicates an edema of the ocular tissues, a sign of eye irritation, probably due to exudation from abnormally permeable capillaries and a conjunctival vasodilation. It is surprising and unexpected that the LED exposed eye suffers from an important edema without detectable damage to the retina by fundus examination. This also suggests that there are probably invisible photochemical lesions. Actually, our study shows the presence of important oxidative damage, involving proteins and nucleic acids, as well as an important amount of cell death. In 2001, the Dawson's study showed that blue LED (460 nm), and argon laser (458 nm), lead to the same retinal lesions with corneal irradiance of 10 J/cm^2 [27]. These results were confirmed by the Ueda's team that showed retinal damages at the macula with blue LEDs (465 nm) [28]. In every case the used devices were almost experimental, while in the present study we use commercially available sources. Moreover, irradiance flux were about 1/1000 than those used in the Dawson's experiments (our LED induce a corneal irradiance of about 0.0026 J/cm^2). Recently, the study of Mukai *et al* showed that retinas of monkeys exposed to LEDs light for 8 h present intracellular vacuoles in the outer segments of photoreceptors, a feature also seen in our study. This study also show that these structural lesions are accompanied by functional alterations revealed by ERG study showing a decreased response of rods and cones [29], but the mechanisms of the toxicity were not analyzed.

In this study we analyzed the molecular mechanisms of retinal damage. We use the usual model of albinos rat. Although the pertinence of this model and the translation of the results to human being is matter of discussion, it is useful to get an idea of the kind of lesions found with theses new devices as compared with other already investigated in our laboratory [17-18].

Phototoxicity depends mainly on intensity of the radiation, its exposure-time and its spectrum, as showed by Knels's team who used two types of LEDs (411 nm blue and 470 nm green) on a line of R28 retinal cells [30]. This *in vitro* study revealed activation of the antioxidant system involving glutathione in cells illuminated regardless exposition, spectrum and power of LEDs. In our model we also find signs of oxidative stress, as revealed by the increased labeling in HGN and N-Tyr, reflecting the oxidation of DNA/RNA and proteins respectively. This oxidative stress seems to be more important with blue light. In our hands the Cree Royal Blue LED produced a higher degree of protein oxidation (as seen by N-Tyr western blot) than the other blue LEDs, although the dose of exposure were quite similar (e.g. 42.3 J/cm² for Nichia blue and 34.2 for Cree Royal Blue).

The oxidative stress induces a retinal response unrevealed by a reaction of Müller cells though the increased expression of GFAP, a well known sign of retinal stress (Figure 2 and supplementary figure 5). The increase of GFAP expression is thought to help maintaining the integrity of the macroglial network in stress conditions [31]. The stress generating this reaction could be the oxidative stress *per se*, but also a mechanical stress generated by the intercellular edema that we described (supplementary figure 4).

Another stress response concerns the p62 protein (sequestosome 1). This is a multifunctional ubiquitin-binding scaffolding protein involved in autophagy but also in oxidative stress [32]. It is thought to be a proteotoxic stress response protein [33]. 18 h of white LED exposure induced a nuclear immunostaining of p62 especially in the INL but also in the ONL and GCL. This nuclear translocation of p62 was described as being a disruption of the nuclear-cytoplasmic shuttling of p62 [34]. In order to investigate the role of the blue part of the light spectrum in p62 expression, we used western blotting analysis of illuminated retina after 18 h of LED exposure with green and blue LEDs. We observed an increase of the entire form of p62 with blue LEDs (449, 467 and 473 nm) contrary to green LED (507 nm) and non-exposed retina. Furthermore, we observed cleavage of p62 revealed by two new bands with apparent molecular weights of 46 kDa and 37 kDa. These N-terminal fragments of p62 correspond to the cleavage by caspase 8 which seems to occur when there is autophagy impairment, a state that promotes apoptosis [35] or autophagic cell death [36]. The immunoreactive bands corresponding to the cleaved fragments are more intense in the retinas illuminated with blue LEDs (449, 467 and 473 nm) with respect to green LED (507 nm), suggesting a stronger alteration of basal autophagy and a stronger promotion of cell death.

The stress generated by LED exposure induces the cell stress responses discussed above, concomitantly with survival promoting signals. Among the possible responses of the retinal cells we investigated the PKC zeta-NFkB axis, because it was shown to be largely involved in other responses to retinal damage, as in diabetic retinopathy [37] and even in light damage (unpublished results). Following stress, activated PKC zeta phosphorylates IKK (Ikappa kinase B), which phosphorylates IKB leading to the release of NFkB and its nuclear translocation [38]. NFkB promotes the transcription of anti-apoptotic genes such as Bcl-2, IAP, TRAF1/2 (TNF receptor-associated factors) [39]. 18 h of LED exposure induced a nuclear immunostaining of phospho-NFkB in the INL and GCL absent in non-exposed retina. The nuclear staining seems to be more intense in INL after the illumination with blue LED (NB, CRB and CB). This result was confirmed by western blotting analysis using the same antibody that recognizes the phosphorylated serine 311 form of NFkB, which is a specific substrate of the PKC zeta pathway [40]. PKC zeta typically has a biphasic response, being protective when activated and promoting cell death when cleaved. Cleavage of PKC zeta corresponds to a constitutive activated form of PKC zeta mediated by the caspase pathway [41-42]. The phosphorylation of threonine 410 of PKC zeta corresponds to the activated enzyme which in turn induces a phosphorylation cascade of other proteins to transducer stress signals. Western blot using phospho-PKC zeta antibody revealed an increase of the phosphorylated PKC zeta (band of 72 kDa) in the retina exposed to blue LEDs (449, 467 and 473 nm) compared to non-exposed retina, suggesting the involvement of PKC zeta pathway in the stress response after exposure. To note, the exposure to the Nichia Blue Green LED produces a different reaction with a cleavage of the enzyme not seen in the other conditions. This fact, together with the presence of many TUNEL positive cells, suggests that the protective signals are overwhelmed triggering cell death.

Among the different forms of cell death, apoptosis is the best known and it has been largely involved in retinal degeneration [9-10]. Although our group and others have shown the lack of caspase activation in light induced retinal degeneration [17, 43], the presence of the PKC zeta fragment suggested caspase activation. We investigate this issue by using an anti active-caspase 3 antibody. Surprisingly, no label was found in the ONL, the layer where the TUNEL positive cells accumulate, but in the INL, where not a single TUNEL positive cell was seen in all the experiments we have performed, not even when using very long times of exposure.

We have then cells that are dying, owing to their TUNEL positivity, but that are active-caspase 3 negative. This kind of situation can be found in caspase independent apoptosis, in

necroptosis or in necrosis. In order to have more insight into this issue, we investigated the state of PARP-1.

PARP-1 is known for its role in DNA repair [44]. During apoptosis, cleavage of PARP-1 by caspases 3 and 7 has become a useful hallmark of this type of cell death [21]. The caspase cleavage of PARP-1 generates a catalytic fragment of 89 kDa and a 24 kDa fragment corresponding to the DNA-binding domain (DBD). Interestingly, PARP-1 is also cleaved during necrosis but in this situation it generates a 62 kDa fragment [22]. After 18 h of exposure to white LEDs, western blot analysis showed different patterns between exposed and unexposed rats. We observed a band with very high molecular weight (250 kDa) corresponding to the automodified PARP-1. Automodification of PARP-1 by poly (ADP-ribose) is involved in its interaction with damaged DNA and it is thought to up-regulate the NFkB/DNA complex [45]. The expression of PARP-1 (113 kDa) is also increased. Moreover, we find the 62 kDa fragment suggesting the existence of a necrotic cell death after LED exposure. Additionally, a band of approximately 44/42 kDa is observed that could be the fragment generated after cleavage of PARP-1 by calpain or cathepsin D, as described by Chaitanya *et al* [24]. These elements support a cell death by necrosis.

To validate the existence of necrosis and evaluate the weight of blue light in its activation we analyzed expression of RIP 1 and RIP 3 kinases by western blot (Figure 8). Both RIP 1 and RIP 3 were slightly increased in all exposed retina. The 42/40 kDa doublets observed were described as the C-terminal death-domain containing portion of RIP 1 kinase [46]. The cleavage of RIP 1 kinase abolishes its anti-apoptotic effect by impairing its capacity to induce NFkB [47]. The study of RIP 3 kinase also revealed a cleaved form of 39 kDa in retina exposed to green LED (NBG). This is a product of caspase 8 that is also activated (Figure 8). It is important to note that cleavage of RIP 3 by caspase 8 inactivates this protein due to the loss of its kinase domain and its ability to form the necrosome, a key stage of necrosis [48]. Due to their interaction with death receptors and their ability to form the necrosome, RIP 1 and RIP 3 kinases control the switch between apoptotic and necrotic cell death [49]. Taken together these results indicate that the greener LED (NBG) tends to induce apoptotic cell death, while the blue radiation tends to induce necrotic cell death (CRB and CB). We further explore this point by analyzing caspase independent effectors of cell death like AIF [16] and LEI/L-DNase II [50]. Both effectors were modestly activated in ONL during early exposure, while L-DNase II seems massively activated at later times (24 h). This is not

surprising since this system is usually activated by metabolic stress [51]. It is also interesting to note that AIF and L-DNase II activation can be mediated by the activation of calpain 1, the first directly, by cleavage and release from the mitochondrial inner membrane [52-53], the second indirectly by permeabilizing lysosomes and releasing cathepsin D [54]. Moreover, although theses effectors have originally been described as mediating apoptosis, AIF has been shown to mediate necroptosis [55] and LEI/L-DNase II, due to its activation by lysosomal enzymes, could be also an effector of necrosis [56].

We further investigated the presence of necrosis by staining cells with PI. This DNA binding dye is very useful in characterizing cell death. It is used in routine in flow cytometry because of its capacity to enter the cell and label DNA when the plasma membrane is damaged. We performed then an intravitreal injection of this dye some minutes before the sacrifice of the animal. Interestingly, a very high number of photoreceptors were labeled, much more than photoreceptors that are TUNEL positive; indicating that permeabilization of the plasma membrane precedes degradation of DNA.

The existence of this necrosis easily explains the presence of retinal edema seen in the histological sections, an edema that is not sub-retinal but interstitial. This could also explain the presence of an early inflammatory reaction, probably due to the release of DAMPS (damage-associated molecular-pattern molecules) [57] that may also be responsible for the chemosis seen in the exposed rats.

Using a comparable set of experiments Shang's team recently show that white LEDs lead to photoreceptors death [58], with an important oxidative stress, as we confirmed in this paper, however, according to our data, apoptosis is not the major pathway involved in photoreceptor demise. Actually, the experimental design of Shang's *et al* has several differences with ours but two differences are very important: first they use dark adapted animals, a procedure that increases retinal sensitivity to light. Second, they evaluate the retinal damage after a recovery period, allowing the tissue to eventually repair. In our experimental set-up we analyzed the eyes just after exposure in order to investigate the mechanism of cell death activated during degeneration.

Taken together these data indicate that the blue component of the LED is the major cause of retinal damage, as has been previously predicted [12]. In addition, current regulation

establishes that for an exposure greater than 10 000 s, ELV, expressed in term of blue light radiance is about 100 W/m²/sr [14], largely over the radiances used in this study (table 1), suggesting that these regulations should be re-evaluated.

Moreover, the reduced size of LEDs allows the production of composite sources of very high luminance. This introduces a cautionary note on their use in domestic lighting that needs to be extremely controlled to remain safe for the vision.

Acknowledgments: This work was supported by INSERM, ENVA, CSTB and by an ADEME financial support (RETINALED project). IJ has a fellowship from ADEME. Authors are in debt with Dr. Patricia Lassiaz for helpful discussions on PKC zeta and with Mrs Brigitte Goldenberg and Mr. Christophe Klein for technical assistance.

References:

[1] Cheung, L. K.; Eaton, A. Age-related macular degeneration. *Pharmacotherapy* **33:**838-855; 2013.

[2] Paskowitz, D. M.; LaVail, M. M.; Duncan, J. L. Light and inherited retinal degeneration. *Br J Ophthalmol* **90:**1060-1066; 2006.

[3] Blasiak, J.; Salminen, A.; Kaarniranta, K. Potential of epigenetic mechanisms in AMD pathology. *Front Biosci (Schol Ed)* **5:**412-425; 2013.

[4] Sui, G. Y.; Liu, G. C.; Liu, G. Y.; Gao, Y. Y.; Deng, Y.; Wang, W. Y.; Tong, S. H.; Wang, L. Is sunlight exposure a risk factor for age-related macular degeneration? A systematic review and meta-analysis. *Br J Ophthalmol* **97:**389-394; 2013.

[5] Hirai, F. E.; Moss, S. E.; Knudtson, M. D.; Klein, B. E.; Klein, R. Retinopathy and survival in a population without diabetes: The Beaver Dam Eye Study. *Am J Epidemiol* **166:**724-730; 2007.

[6] Klein, R.; Klein, B. E.; Knudtson, M. D.; Meuer, S. M.; Swift, M.; Gangnon, R. E. Fifteen-year cumulative incidence of age-related macular degeneration: the Beaver Dam Eye Study. *Ophthalmology* **114:**253-262; 2007.

[7] Noell, W. K.; Walker, V. S.; Kang, B. S.; Berman, S. Retinal damage by light in rats. *Invest Ophthalmol* **5:**450-473; 1966.

[8] Organisciak, D. T.; Darrow, R. A.; Barsalou, L.; Darrow, R. M.; Lininger, L. A. Light-induced damage in the retina: differential effects of dimethylthiourea on photoreceptor survival, apoptosis and DNA oxidation. *Photochem Photobiol* **70:**261-268; 1999.

[9] Reme, C. E.; Grimm, C.; Hafezi, F.; Wenzel, A.; Williams, T. P. Apoptosis in the Retina: The Silent Death of Vision. *News Physiol Sci* **15:**120-124; 2000.

[10] Reme, C. E.; Grimm, C.; Hafezi, F.; Marti, A.; Wenzel, A. Apoptotic cell death in retinal degenerations. *Prog Retin Eye Res* **17:**443-464; 1998.

[11] Behar-Cohen, F.; Martinsons, C.; Vienot, F.; Zissis, G.; Barlier-Salsi, A.; Cesarini, J. P.; Enouf, O.; Garcia, M.; Picaud, S.; Attia, D. Light-emitting diodes (LED) for domestic lighting: any risks for the eye? *Prog Retin Eye Res* **30:**239-257; 2011.

[12] van Norren, D.; Gorgels, T. G. The action spectrum of photochemical damage to the retina: a review of monochromatic threshold data. *Photochem Photobiol* **87:**747-753; 2011.

[13] Torriglia, A.; Chaudun, E.; Chany-Fournier, F.; Jeanny, J. C.; Courtois, Y.; Counis, M. F. Involvement of DNase II in nuclear degeneration during lens cell differentiation. *J Biol Chem* **270:**28579-28585; 1995.

[14] Matthes, R.; Feychting, M.; Ahlbom, A.; Breitbart, E.; Croft, R.; de Gruijl, F.; Green, A.; Hietanen, M.; Jokela, K.; Lin, J. Icnirp guidelines on limits of exposure to incoherent visible and infrared radiation. *Health Physics* **105:**74-91; 2013.

[15] Huxlin, K. R.; Dreher, Z.; Schulz, M.; Dreher, B. Glial reactivity in the retina of adult rats. *Glia* **15:**105-118; 1995.

[16] Susin, S. A.; Lorenzo, H. K.; Zamzami, N.; Marzo, I.; Snow, B. E.; Brothers, G. M.; Mangion, J.; Jacotot, E.; Costantini, P.; Loeffler, M.; Larochette, N.; Goodlett, D. R.; Aebersold, R.; Siderovski, D. P.; Penninger, J. M.; Kroemer, G. Molecular characterization of mitochondrial apoptosis-inducing factor. *Nature* **397:**441-446; 1999.

[17] Chahory, S.; Keller, N.; Martin, E.; Omri, B.; Crisanti, P.; Torriglia, A. Light induced retinal degeneration activates a caspase-independent pathway involving cathepsin D. *Neurochem Int* **57:**278-287; 2010.

[18] Chahory, S.; Padron, L.; Courtois, Y.; Torriglia, A. The LEI/L-DNase II pathway is activated in light-induced retinal degeneration in rats. *Neurosci Lett* **367:**205-209; 2004.

[19] Padron-Barthe, L.; Lepretre, C.; Martin, E.; Counis, M. F.; Torriglia, A. Conformational modification of serpins transforms leukocyte elastase inhibitor into an endonuclease involved in apoptosis. *Mol Cell Biol* **27:**4028-4036; 2007.

[20] Galluzzi, L.; Kepp, O.; Kroemer, G. RIP kinases initiate programmed necrosis. *J Mol Cell Biol* **1:**8-10; 2009.

[21] Kaufmann, S. H.; Desnoyers, S.; Ottaviano, Y.; Davidson, N. E.; Poirier, G. G. Specific proteolytic cleavage of poly(ADP-ribose) polymerase: an early marker of chemotherapy-induced apoptosis. *Cancer Res* **53:**3976-3985; 1993.

[22] Gobeil, S.; Boucher, C. C.; Nadeau, D.; Poirier, G. G. Characterization of the necrotic cleavage of poly(ADP-ribose) polymerase (PARP-1): implication of lysosomal proteases. *Cell Death Differ* **8:**588-594; 2001.

[23] Boucher, C.; Gobeil, S.; Samejima, K.; Earnshaw, W. C.; Poirier, G. G. Identification and analysis of caspase substrates: proteolytic cleavage of poly(ADP-ribose)polymerase and DNA fragmentation factor 45. *Methods Cell Biol* **66:**289-306; 2001.

[24] Chaitanya, G. V.; Steven, A. J.; Babu, P. P. PARP-1 cleavage fragments: signatures of cell-death proteases in neurodegeneration. *Cell Commun Signal* **8:**31; 2010.

[25] Shi, J.; Wong, J.; Piesik, P.; Fung, G.; Zhang, J.; Jagdeo, J.; Li, X.; Jan, E.; Luo, H. Cleavage of sequestosome 1/p62 by an enteroviral protease results in disrupted selective autophagy and impaired NFKB signaling. *Autophagy* **9:**1591-1603; 2013.

[26] Martinsons, C.; Zissis, G. Potential Health Issues of Solid-State Lighting », Report of the International Energy Agency, Energy Efficient End-Use Equipment (4E), SSL Annex,. *http://ssl.iea-4e.org/task-1-quality-assurance/health-aspects-report*; 2014.

[27] Dawson, W.; Nakanishi-Ueda, T.; Armstrong, D.; Reitze, D.; Samuelson, D.; Hope, M.; Fukuda, S.; Matsuishi, M.; Ozawa, T.; Ueda, T.; Koide, R. Local fundus response to blue (LED and laser) and infrared (LED and laser) sources. *Exp Eye Res* **73:**137-147; 2001.

[28] Ueda, T.; Nakanishi-Ueda, T.; Yasuhara, H.; Koide, R.; Dawson, W. W. Eye damage control by reduced blue illumination. *Exp Eye Res* **89:**863-868; 2009.

[29] Mukai, R.; Akiyama, H.; Tajika, Y.; Shimoda, Y.; Yorifuji, H.; Kishi, S. Functional and morphologic consequences of light exposure in primate eyes. *Invest Ophthalmol Vis Sci* **53:**6035-6044; 2012.

[30] Knels, L.; Valtink, M.; Roehlecke, C.; Lupp, A.; de la Vega, J.; Mehner, M.; Funk, R. H. Blue light stress in retinal neuronal (R28) cells is dependent on wavelength range and irradiance. *Eur J Neurosci* **34:**548-558; 2011.

[31] Lundkvist, A.; Reichenbach, A.; Betsholtz, C.; Carmeliet, P.; Wolburg, H.; Pekny, M. Under stress, the absence of intermediate filaments from Müller cells in the retina has structural and functional consequences. *Journal of cell science* **117:**3481-3488; 2004.

[32] Nezis, I. P.; Stenmark, H. p62 at the interface of autophagy, oxidative stress signaling, and cancer. *Antioxid Redox Signal* **17:**786-793; 2012.

[33] Geetha, T.; Wooten, M. W. Structure and functional properties of the ubiquitin binding protein p62. *FEBS Lett* **512:**19-24; 2002.

[34] Pankiv, S.; Lamark, T.; Bruun, J. A.; Overvatn, A.; Bjorkoy, G.; Johansen, T. Nucleocytoplasmic shuttling of p62/SQSTM1 and its role in recruitment of nuclear polyubiquitinated proteins to promyelocytic leukemia bodies. *J Biol Chem* **285:**5941-5953; 2010.

[35] Norman, J. M.; Cohen, G. M.; Bampton, E. T. The in vitro cleavage of the hAtg proteins by cell death proteases. *Autophagy* **6:**1042-1056; 2010.

[36] Giansanti, V.; Rodriguez, G. E.; Savoldelli, M.; Gioia, R.; Forlino, A.; Mazzini, G.; Pennati, M.; Zaffaroni, N.; Scovassi, A. I.; Torriglia, A. Characterization of stress response in human retinal epithelial cells. *J Cell Mol Med* **17:**103-115; 2013.

[37] Omri, S.; Behar-Cohen, F.; Rothschild, P. R.; Gelize, E.; Jonet, L.; Jeanny, J. C.; Omri, B.; Crisanti, P. PKCzeta mediates breakdown of outer blood-retinal barriers in diabetic retinopathy. *PLoS One* **8:**e81600; 2013.

[38] Hirai, T.; Chida, K. Protein kinase Czeta (PKCzeta): activation mechanisms and cellular functions. *J Biochem* **133:**1-7; 2003.

[39] Li, X.; Stark, G. R. NFkappaB-dependent signaling pathways. *Exp Hematol* **30:**285-296; 2002.

[40] Duran, A.; Diaz-Meco, M. T.; Moscat, J. Essential role of RelA Ser311 phosphorylation by zetaPKC in NF-kappaB transcriptional activation. *EMBO J* **22:**3910-3918; 2003.

[41] Smith, L.; Chen, L.; Reyland, M. E.; DeVries, T. A.; Talanian, R. V.; Omura, S.; Smith, J. B. Activation of atypical protein kinase C zeta by caspase processing and degradation by the ubiquitin-proteasome system. *J Biol Chem* **275:**40620-40627; 2000.

[42] Smith, L.; Smith, J. B. Lack of constitutive activity of the free kinase domain of protein kinase C zeta. Dependence on transphosphorylation of the activation loop. *J Biol Chem* **277:**45866-45873; 2002.

[43] Donovan, M.; Carmody, R. J.; Cotter, T. G. Light-induced photoreceptor apoptosis in vivo requires neuronal nitric-oxide synthase and guanylate cyclase activity and is caspase-3-independent. *J Biol Chem* **276:**23000-23008; 2001.

[44] Dantzer, F.; Schreiber, V.; Niedergang, C.; Trucco, C.; Flatter, E.; De La Rubia, G.; Oliver, J.; Rolli, V.; Menissier-de Murcia, J.; de Murcia, G. Involvement of poly(ADP-ribose) polymerase in base excision repair. *Biochimie* **81:**69-75; 1999.

[45] Nakajima, H.; Nagaso, H.; Kakui, N.; Ishikawa, M.; Hiranuma, T.; Hoshiko, S. Critical role of the automodification of poly(ADP-ribose) polymerase-1 in nuclear factor-kappaB-dependent gene expression in primary cultured mouse glial cells. *J Biol Chem* **279:**42774-42786; 2004.

[46] Lin, Y.; Devin, A.; Rodriguez, Y.; Liu, Z. G. Cleavage of the death domain kinase RIP by caspase-8 prompts TNF-induced apoptosis. *Genes Dev* **13:**2514-2526; 1999.

[47] Ting, A. T.; Pimentel-Muinos, F. X.; Seed, B. RIP mediates tumor necrosis factor receptor 1 activation of NF-kappaB but not Fas/APO-1-initiated apoptosis. *EMBO J* **15:**6189-6196; 1996.

[48] Moriwaki, K.; Chan, F. K. RIP3: a molecular switch for necrosis and inflammation. *Genes Dev* **27:**1640-1649; 2013.

[49] Cho, Y. S.; Challa, S.; Moquin, D.; Genga, R.; Ray, T. D.; Guildford, M.; Chan, F. K. Phosphorylation-driven assembly of the RIP1-RIP3 complex regulates programmed necrosis and virus-induced inflammation. *Cell* **137:**1112-1123; 2009.

[50] Torriglia, A.; Perani, P.; Brossas, J. Y.; Chaudun, E.; Treton, J.; Courtois, Y.; Counis, M. F. L-DNase II, a molecule that links proteases and endonucleases in apoptosis, derives from the ubiquitous serpin leukocyte elastase inhibitor. *Mol Cell Biol* **18:**3612-3619; 1998.

[51] Altairac, S.; Zeggai, S.; Perani, P.; Courtois, Y.; Torriglia, A. Apoptosis induced by Na+/H+ antiport inhibition activates the LEI/L-DNase II pathway. *Cell Death Differ* **10:**548-557; 2003.

[52] Moubarak, R. S.; Yuste, V. J.; Artus, C.; Bouharrour, A.; Greer, P. A.; Menissier-de Murcia, J.; Susin, S. A. Sequential activation of poly(ADP-ribose) polymerase 1, calpains, and Bax is essential in apoptosis-inducing factor-mediated programmed necrosis. *Mol Cell Biol* **27:**4844-4862; 2007.

[53] Norberg, E.; Gogvadze, V.; Ott, M.; Horn, M.; Uhlen, P.; Orrenius, S.; Zhivotovsky, B. An increase in intracellular Ca2+ is required for the activation of mitochondrial calpain to release AIF during cell death. *Cell Death Differ* **15:**1857-1864; 2008.

[54] Villalpando Rodriguez, G. E.; Torriglia, A. Calpain 1 induce lysosomal permeabilization by cleavage of lysosomal associated membrane protein 2. *Biochim Biophys Acta* **1833:**2244-2253; 2013.

[55] Baritaud, M.; Cabon, L.; Delavallee, L.; Galan-Malo, P.; Gilles, M. E.; Brunelle-Navas, M. N.; Susin, S. A. AIF-mediated caspase-independent necroptosis requires ATM and DNA-PK-induced histone H2AX Ser139 phosphorylation. *Cell Death Dis* **3:**e390; 2012.

[56] Vanden Berghe, T.; Vanlangenakker, N.; Parthoens, E.; Deckers, W.; Devos, M.; Festjens, N.; Guerin, C. J.; Brunk, U. T.; Declercq, W.; Vandenabeele, P. Necroptosis, necrosis and secondary necrosis converge on similar cellular disintegration features. *Cell Death Differ* **17:**922-930; 2010.

[57] Rubartelli, A.; Lotze, M. T. Inside, outside, upside down: damage-associated molecular-pattern molecules (DAMPs) and redox. *Trends Immunol* **28:**429-436; 2007.

[58] Shang, Y. M.; Wang, G. S.; Sliney, D.; Yang, C. H.; Lee, L. L. White light-emitting diodes (LEDs) at domestic lighting levels and retinal injury in a rat model. *Environ Health Perspect* **122:**269-276; 2014.

Captions to figures:

Table1: Physical parameters of the used LEDs.

LED name: commercial name of the used LED, Wavelength: pick of emission (white LED presents two picks), Luminance: light intensity per surface unit; (candela per square meter) corresponding to our experimental setting; Radiance: reflected, transmitted and emitted energy per surface unit (watt per square meter per steradian). The data presented here correspond to our measurements and experimental settings. The calculations were performed according to "supplementary information 1".

Table 2: Antibodies used in this work.

List of antibodies used for immunohistochemistry (IHC) and Western Blot (WB).

Figure 1: Inflammatory response after white LED exposure.
Male Wistar rats aged 7 weeks (n=4) were exposed to Xanlite XXX Evolution 5W for 1 and 3 days, receiving the estimated retinal dose of light indicated. At the end of the exposure period the eyes were included in optimal cutting temperature medium (Tissue Tek), cryosectioned and immunostained with anti-CD11b (green) or anti-Iba 1 (red), nuclei were counterstained with DAPI (blue). ONL: Outer Nuclear Layer; INL: Inner Nuclear Layer. Scale bar represents 20 µm.

Figure 2: Oxidative stress response after white LED exposure.
Male Wistar rats aged 7 weeks (n=4) were exposed to Xanlite XXX Evolution 5W for 18 h, receiving the estimated retinal dose of light indicated. At the end of the exposure period the eyes were included in optimal cutting temperature medium (Tissue Tek),, cryosectioned and immunostained with anti-8-hydroxy-guanosine (HGN), anti-nitro-tyrosine (N-Tyr), anti-sequestosome (p62) or anti-Glial Fibrillary Acid Protein (GFAP). ONL indicates the outer nuclear layer, INL the Inner nuclear layer. Scale bar represents 20 µm.

Figure 3: The mechanisms of cell death in retina after white LED exposure.
Male Wistar rats aged 7 weeks (n=4) were exposed to Xanlite XXX Evolution 5W for 18 h. NE: Non exposed rats, WL: rats exposed to white LEDs, 125 J/cm². At the end of the

exposure period the eyes were analyzed regarding different effectors of cell death. **A:** Eyes were stained with the TUNEL assay (TUNEL) or immunostained with anti-active-caspase 3 (Caspase 3), anti-apoptosis inducing factor (AIF), anti-LEI derived DNase II (LEI/L-DNase II), anti-receptor interacting protein (RIP 1) or anti-receptor interacting protein kinase (RIP 3). Black vertical bars represent ONL. Scale bar represents 20 µm. **B:** The outer nuclear layer was further analyzed by triple staining by confocal microscopy: upper panel: anti-lamin B in green, anti-AIF in red and DAPI in blue. In lower panel the red fluorescence corresponds to anti-LEI/L-DNase II. Black vertical bars represent ONL. Scale bar represents 0.5 µm. **C:** after light exposure the eyes were enucleated, the retina dissected, extracted with Laemmli sample buffer and loaded on the top of a 10% SDS-PAGE, transferred onto a nitrocellulose membrane and probed for PARP-1. A control of charge has been made using an anti-actin on the same membrane after striping (actin).

Figure 4: structural modifications of the retina examined by transmittance electron microscopy (TEM).

Male Wistar rats aged 7 weeks (n=4) were exposed to Xanlite XXX Evolution 5W for 18 h. At the end of the exposure period the eyes were analyzed by TEM. NE, non exposed animals, WL: exposed animals to white LED (125 J/cm^2). ROS: rod outer segments, PRN: photoreceptor nuclear layer also called ONL. RIS: rod inner segment layer. In PRN panels white arrow head shows dilated interphotoreceptors spaces, black arrow an apoptotic cell and white arrows necrotic nuclei. RIS panels: arrow head indicates dilated mitochondria, black arrow dilated endoplasmic reticulum. Scale bar represents 0.5 µm.

Figure 5: Oxidative stress response after blue LED exposure.

Male Wistar rats aged 7 weeks (n=4) were exposed to Nichia Blue Green LEDs (NBG), Nichia Blue LEDs (NB), Cree Blue LEDs (CB) or Cree Royal Blue LEDs (CRB) for 18 h. NE: non exposed animals. **A:** shows the immunoreactivity of the retinas using an anti-8-hydroxy-guanosine (HGN) or an anti nitro-tyrosine (N-Tyr) antibodies. Scale bar represents 20 µm. **B:** after light exposure the eyes were enucleated, the retina dissected, extracted with M-PER (Pierce) buffer and loaded on the top of a 12% SDS-PAGE, transferred onto a nitrocellulose membrane and probed for nitro-tyrosine. Ponceau Red (PR) labeling was used as a charge control.

Figure 6: Western Blot analysis of retinas from animals exposed to blue LEDs.

Male Wistar rats aged 7 weeks (n=4) were exposed to Nichia Blue Green LEDs (NBG), Nichia Blue LEDs (NB), Cree Blue LEDs (CB) or Cree Royal Blue LEDs (CRB) for 18 h. NE: non exposed animals. After light exposure the eyes were enucleated, the retina dissected, extracted with M-PER (Pierce) buffer and loaded on the top of a 12% SDS-PAGE, transferred onto a nitrocellulose membrane and probed with different antibodies. **A:** anti-p62: FL p62 indicates the full length molecule, fragment indicates the cleaved molecule. PR indicates Ponceau Red staining. **B:** anti-PKC zeta: The upper panel was made using an anti-PKC zeta. Full length and cleaved species are indicated. Middle panel was performed using an anti-PPKC zeta (phospho Thr 410). The lower panel is a charge control using actin. **C:** the western blot membrane was probed with anti-phospho-NFkB, ser 311. These are representative results of three independent experiments. PR indicates Ponceau Red staining.

Figure 7: The induction of classical apoptosis in blue LED exposed retinas.

Male Wistar rats aged 7 weeks (n=4) were exposed to Nichia Blue Green LEDs (NBG), Nichia Blue LEDs (NB), Cree Blue LEDs (CB) or Cree Royal Blue LEDs (CRB) for 18. At the end of the exposure period the eyes were analyzed using the TUNEL assay (green) and anti active-caspase 3 (red). INL: Inner nuclear layer, ONL: outer nuclear layer. Scale bar represents 20 µm.

Figure 8: The mechanisms of cell death in retina after blue LED exposure.

Male Wistar rats aged 7 weeks (n=4) were exposed to Nichia Blue Green LEDs (NBG), Nichia Blue LEDs (NB), Cree Blue LEDs (CB) or Cree Royal Blue LEDs (CRB) for 18 h. NE: non exposed animals. At the end of the exposure period the eyes were analyzed regarding different effectors of cell death. **A:** after light exposure the eyes were enucleated, the retina dissected, extracted with M-PER buffer and loaded on the top of a 12% SDS-PAGE, transferred onto a nitrocellulose membrane and probed for apoptosis inducing factor (AIF) (upper panel), LEI derived DNase II (LEI/L-DNase II) (middle panel). In both panels the arrow head indicates the cleaved and therefore activated molecule. The lower panel indicates the quantification of the active L-DNase II as compared to LEI, its precursor. Ponceau red staining was used as the loading control. **B**: same experiment that in panel A using anti-receptor interacting protein 1 and 3 (RIP 1 and RIP 3 respectively) (upper and middle panels) or anti-caspase 8 (lower panel). The arrow heads indicate the cleaved forms of the different molecular species. PR indicates Ponceau Red staining. **C**: After an intra vitreal injection of propidium iodide (PI) the eyes were fixed, cryosectioned and examined under a fluorescence

microscope. Bright nuclei belong to necrotic cells. The lower panel shows the same experiment in which a TUNEL assay has been performed after cryosection. Scale bar represents 20 µm. **D**: after exposure to white LED for 18 h the eyes were enucleated, the retina dissected, extracted with M-PER buffer and loaded on the top of a 12% SDS-PAGE, transferred onto a nitrocellulose membrane and probed RIP 3, caspase 8, p62 and phospho-NFkB. Actin was used as a charge control.

Captions to Supplementary figures:

Supplementary figure 1: Emission spectra of the different LED in W/m² as a function of the emission wavelength.

A: white LED: Xanlite XXX Evolution. Maxima emission: 460 and 600 nm. **B**: Nichia blue-green NCSE 119 A, 507 nm. C: Nichia Blue NCBS 119, 467 nm. **D:** Cree Blue XP-E 473 nm. **E**: Cree Royal Blue XP-E, 449 nm.

Red curve represents the raw emission spectrum; the blue curve represents the actinic spectra, corresponding to the light likely to produce photobiological effects (in this case the irradiance includes a factor Bλ, corresponding to a photobiological risk coefficient. It is a Gaussian curve with a maximum at 440 nm) and the green curve represents the photopic effect, that reflects the efficient amount of light for the eye (it depends of the absorption of the photopigments and it is called Vλ, it is a Gaussian curve with a maximum at 550 nm).

Supplementary figure 2: blue LED device.

A: The four blue LEDs were mounted by groups in order to get an equivalent lightering for each one. **B**: Blue LED device in a working condition.

Supplementary figure 3: Wistar rats exposed to white LED for 24 h.

A: Lateral and top pictures of control rats. **B**: same pictures of rats exposed to white LEDs for 24 h. Black arrow shows chemosis, black arrow head indicates cheek edema.

Supplementary figure 4: Semi-thin sections of rat retina.

Male Wistar rats aged 7 weeks (n=4) were exposed to Xanlite XXX Evolution 5W for 18 h. At the end of the exposure period the eyes were included, sectioned and colored with Toluidine Blue. ONL: Outer Nuclear Layer, ROS: Rod Outer Segment. Scale bar represents 20 µm.

Supplementary figure 5: Kinetics of oxidative stress, retinas exposed to white LEDs.

Male Wistar rats aged 7 weeks (n=4) were exposed to Xanlite XXX Evolution 5W for 6 to 24 h, receiving the indicated retinal dose of light. At the end of the exposure period the eyes were included, sectioned and colored with anti-Glial Fibrillary Acid Protein (GFAP), anti nitro-tyrosine (N-Tyr) or anti-8-hydroxy-guanosine (HGN). ONL indicates the outer nuclear layer, INL the Inner nuclear layer. Scale bar represents 20 µm.

Supplementary figure 6: Thickness of the ONL in retinas exposed to white LEDs.

Male Wistar rats aged 7 weeks (n=4) were exposed to Xanlite XXX Evolution 5W for 1, 2 and 3 days, receiving the retinal dose of light indicated. At the end of the exposure period the eyes were included, cryosectioned and stained with DAPI. ONL indicates the outer nuclear layer, INL the Inner nuclear layer. Scale bar represents 20 µm.

Supplementary figure 7: Labeling with the TUNEL assay of the ONL in retinas exposed to white LEDs.

Male Wistar rats aged 7 weeks (n=4) were exposed to Xanlite XXX Evolution 5W for 1, 2 and 3 days, receiving the retinal dose of light indicated. At the end of the exposure period the eyes were included, cryosectioned and stained with the TUNEL assay. ONL indicates the outer nuclear layer. Scale bar represents 10 µm.

Supplementary figure 8: The mechanisms of cell death in retina after white LED exposure.

Male Wistar rats aged 7 weeks (n=4) were exposed to Xanlite XXX Evolution 5W 1, 2 and 3 days receiving the retinal dose of light indicated. At the end of the exposure period the eyes were included, cryosectioned and stained with anti-apoptosis inducing factor (AIF) and anti-LEI derived DNase II (LEI/L-DNase II). ONL indicates the outer nuclear layer, INL the Inner nuclear layer. Scale bar represents 10 µm.

Supplementary figure 9: The mechanisms of cell response in retina after blue LED exposure.

Male Wistar rats aged 7 weeks (n=4) were exposed to Nichia Blue Green LEDs (NBG), Nichia Blue LEDs (NB), Cree Blue LEDs (CB) or Cree Royal Blue LEDs (CRB) for 18 h. NE: non exposed animals. At the end of the exposure period the eyes were analyzed for PKC

zeta and phospho-NFkB. ONL indicates the outer nuclear layer, INL the Inner nuclear layer. Scale bar represents 20 µm.

Supplementary information 1:

Description of the equations used to calculate the different physical parameters used in our experiments.

–

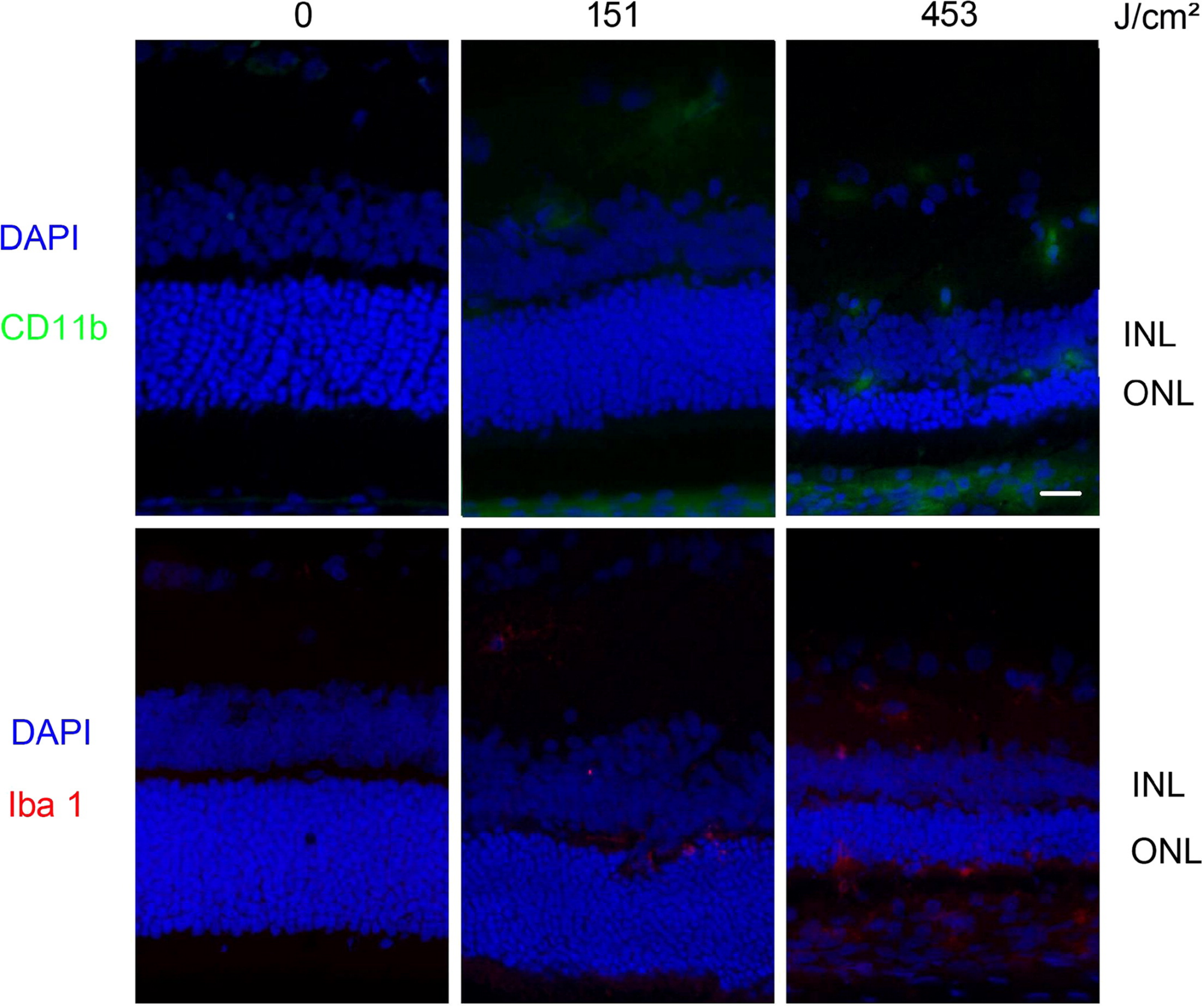
0
151
453
J/cm²
DAPI
CD11b
INL
ONL
DAPI
Iba 1
INL
ONL

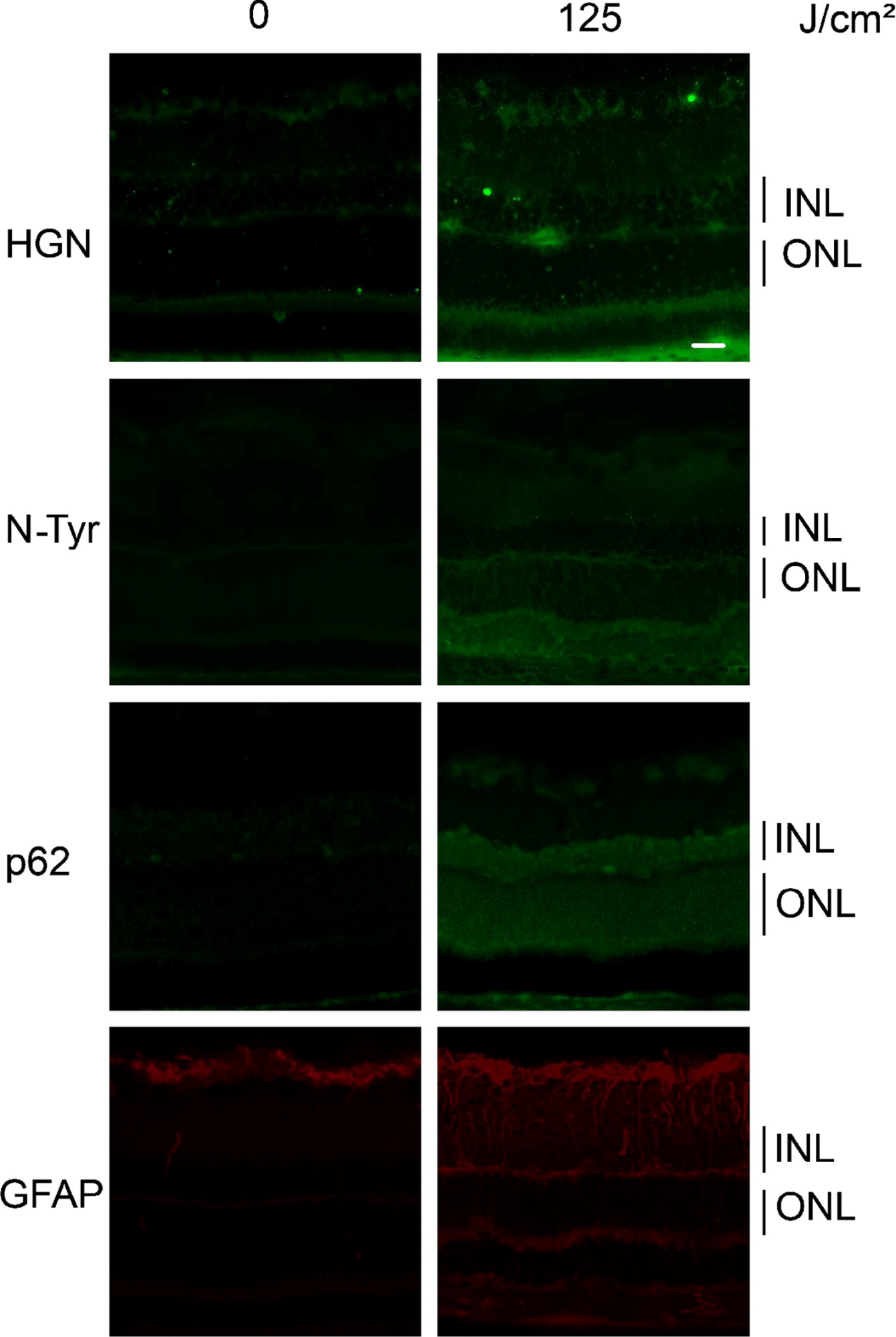
0
125
J/cm²
HGN
INL
ONL
N-Tyr
INL
ONL
p62
INL
ONL
GFAP
INL
ONL

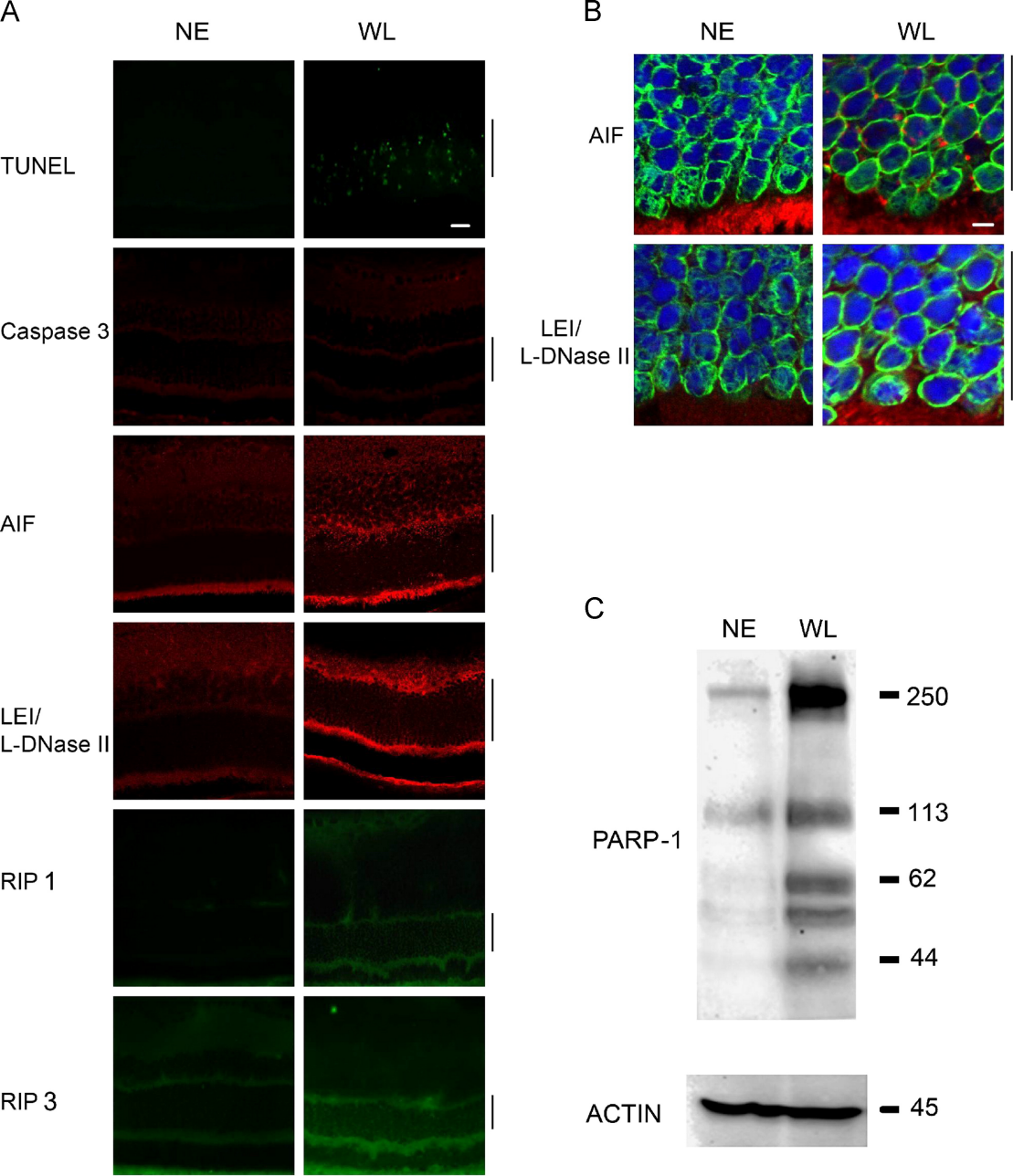
A
NE
WL
TUNEL
Caspase 3
AIF
LEI/
L-DNase II
RIP 1
RIP 3
B
NE
WL
AIF
LEI/
L-DNase II
C
NE
WL
PARP-1
250
113
62
44
ACTIN
45

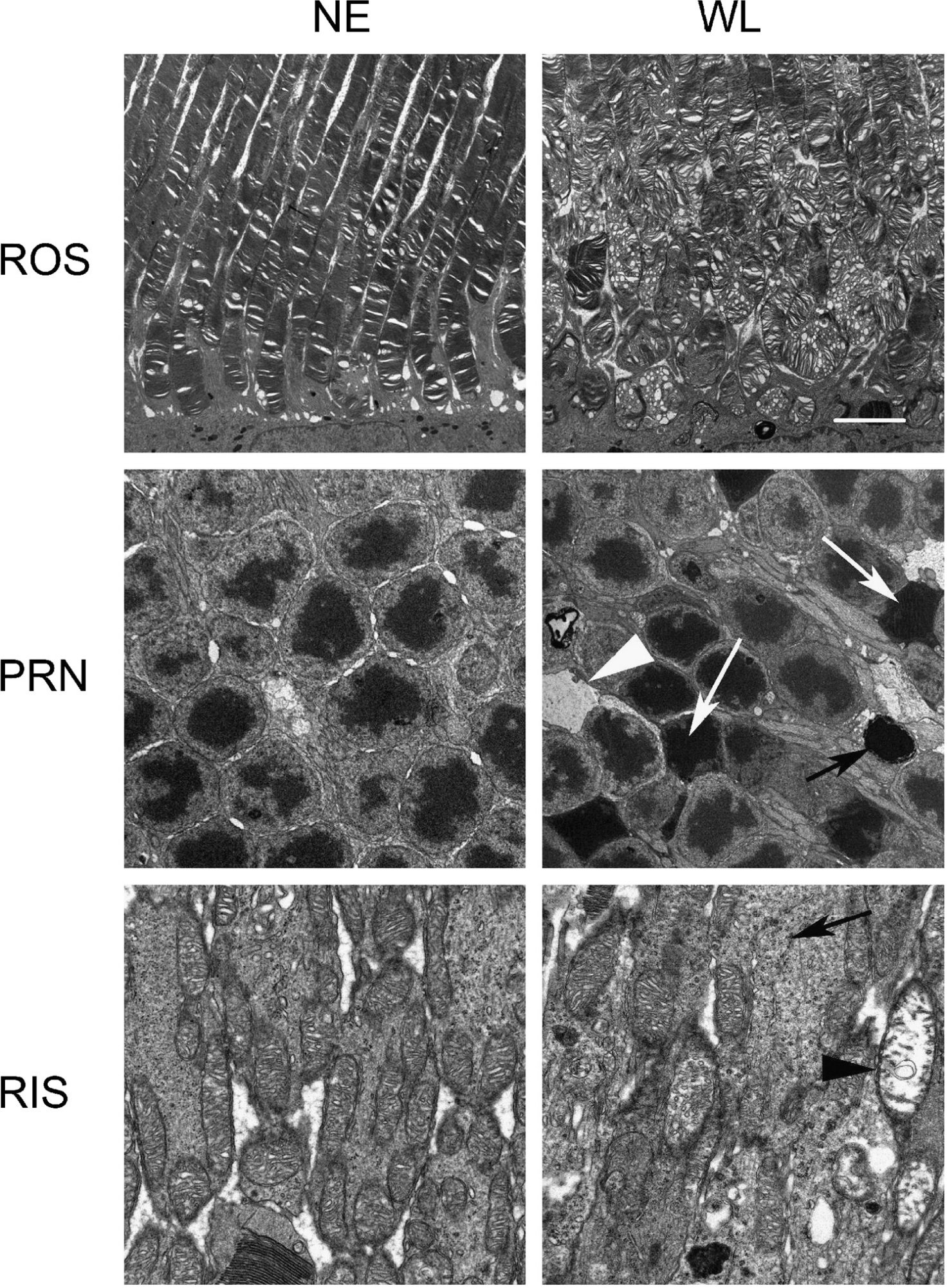
NE
WL
ROS
PRN
RIS

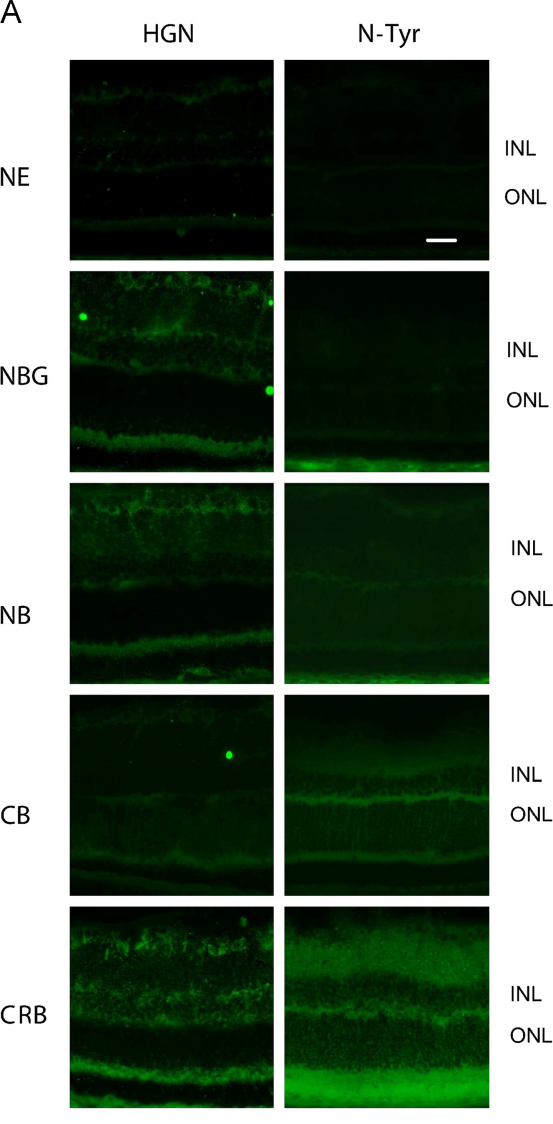
A
HGN
N-Tyr
NE
NBG
NB
CB
CRB
INL
ONL
INL
ONL
INL
ONL
INL
ONL
INL
ONL

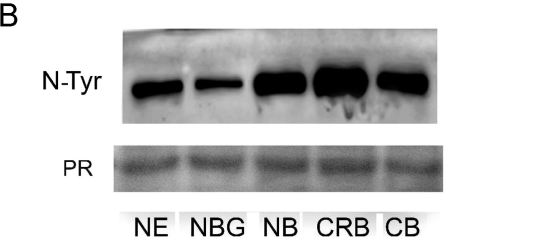
B
N-Tyr
PR
NE
NBG
NB
CRB
CB

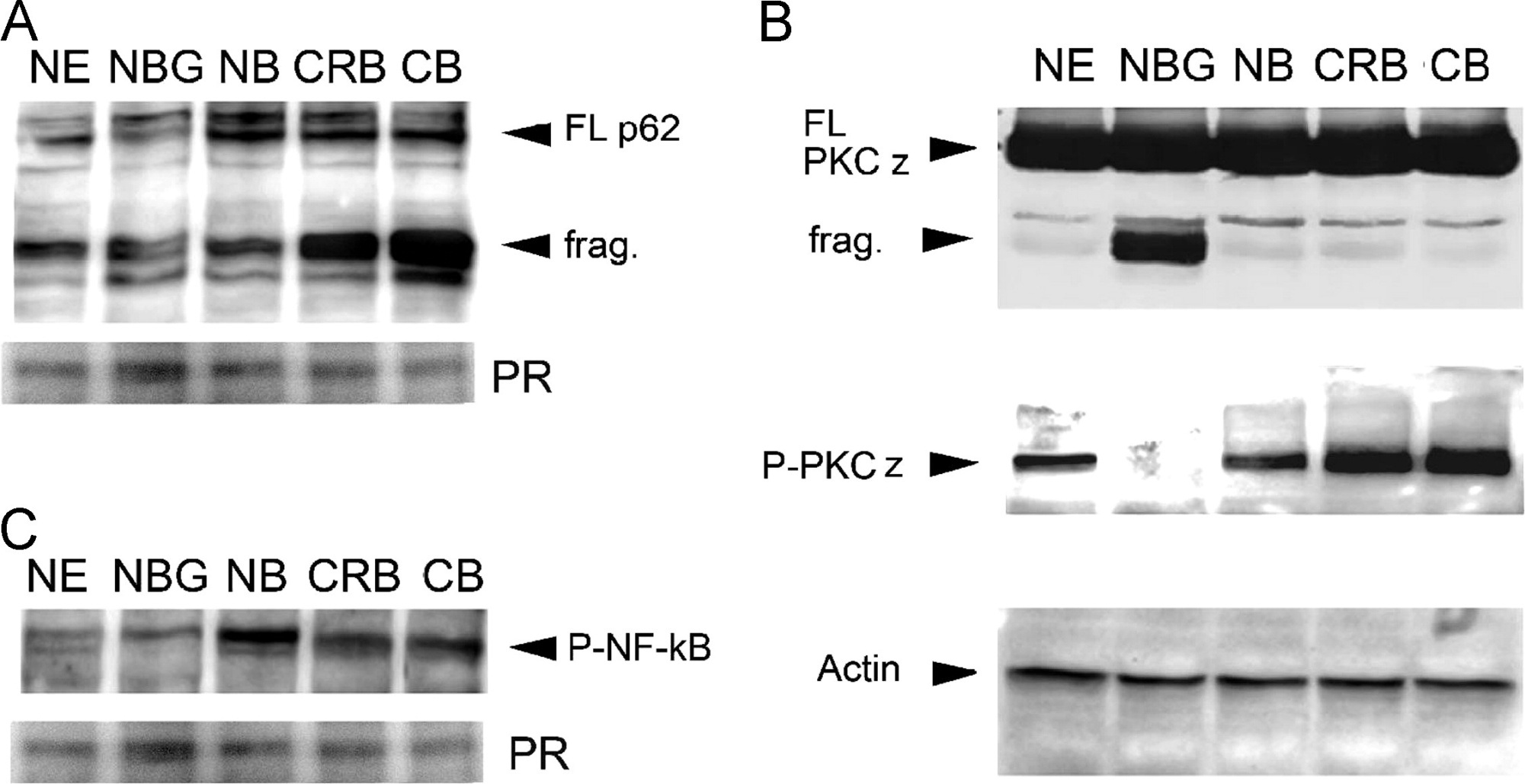
A
NE NBG NB CRB CB
FL p62
frag.
PR
B
NE NBG NB CRB CB
FL
PKC z
frag.
P-PKC z
Actin
C
NE NBG NB CRB CB
P-NF-kB
PR

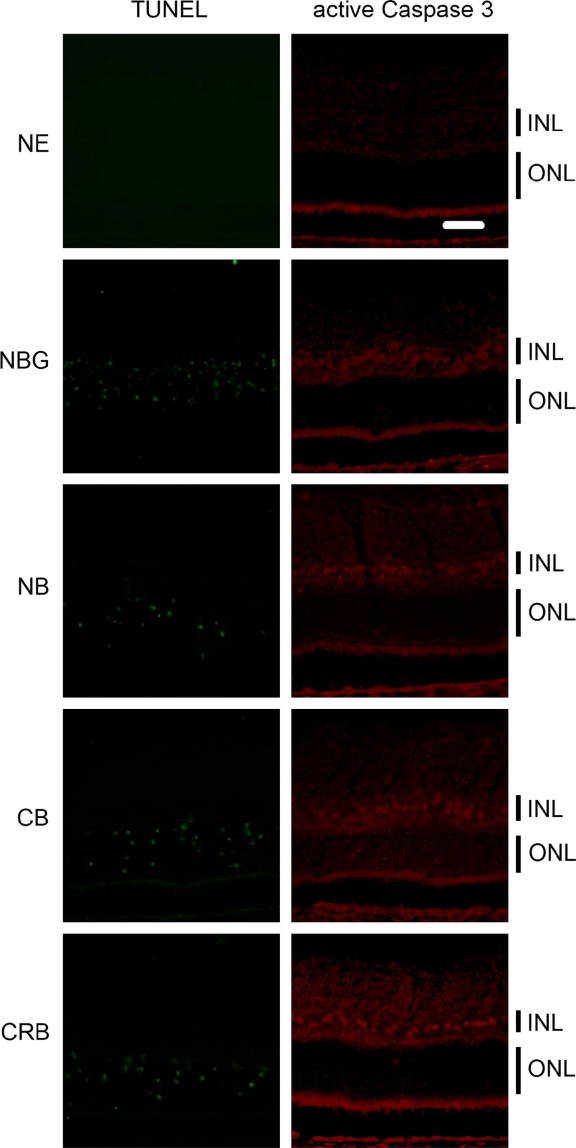
TUNEL
active Caspase 3
NE
NBG
NB
CB
CRB
INL
ONL
INL
ONL
INL
ONL
INL
ONL
INL
ONL

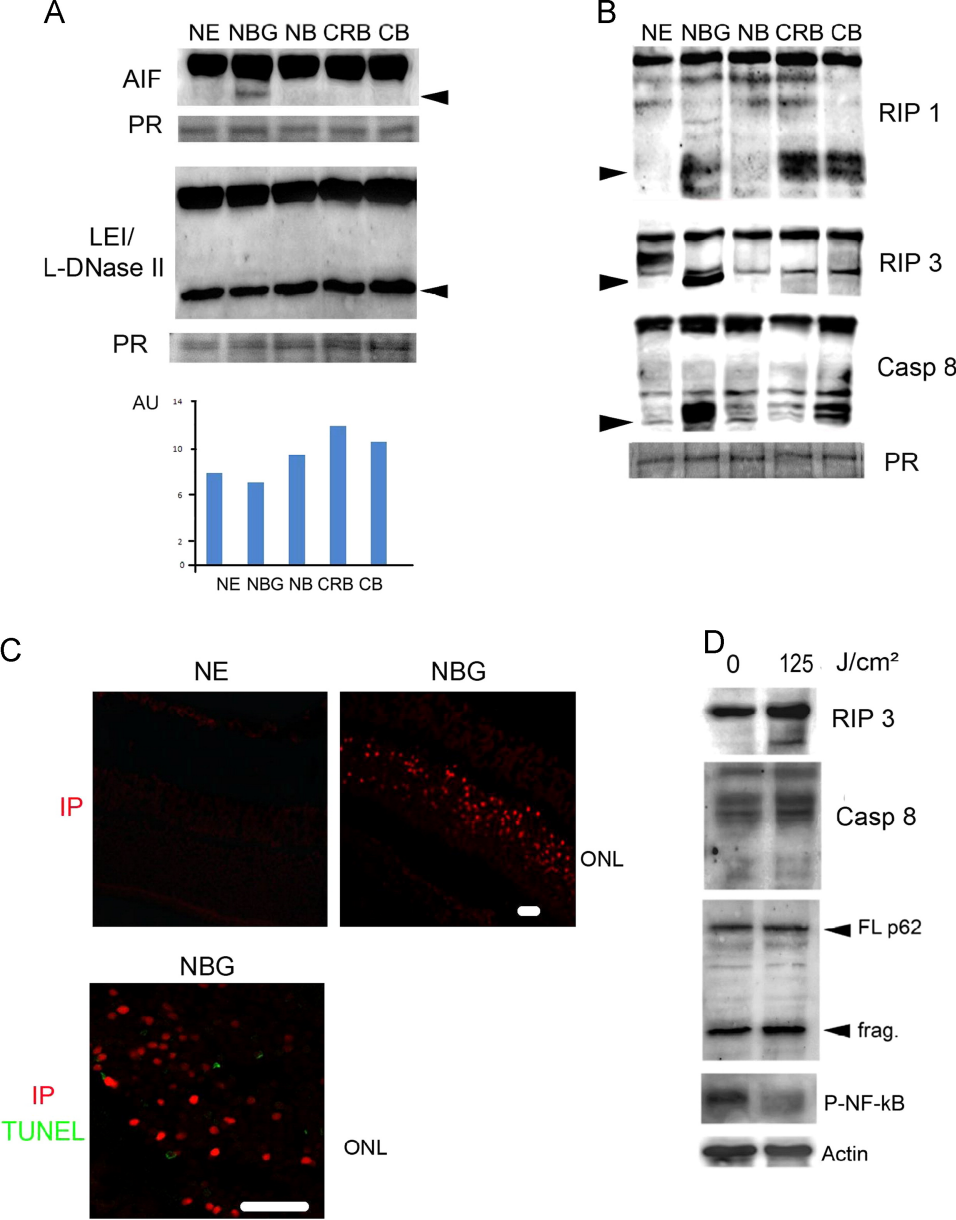
A
NE NBG NB CRB CB
AIF
PR
LEI/
L-DNase II
PR
AU
14
10
6
2
0
NE NBG NB CRB CB
B
NE NBG NB CRB CB
RIP 1
RIP 3
Casp 8
PR
C
NE
NBG
IP
ONL
NBG
IP
TUNEL
ONL
D
0
125
J/cm²
RIP 3
Casp 8
FL p62
frag.
P-NF-kB
Actin

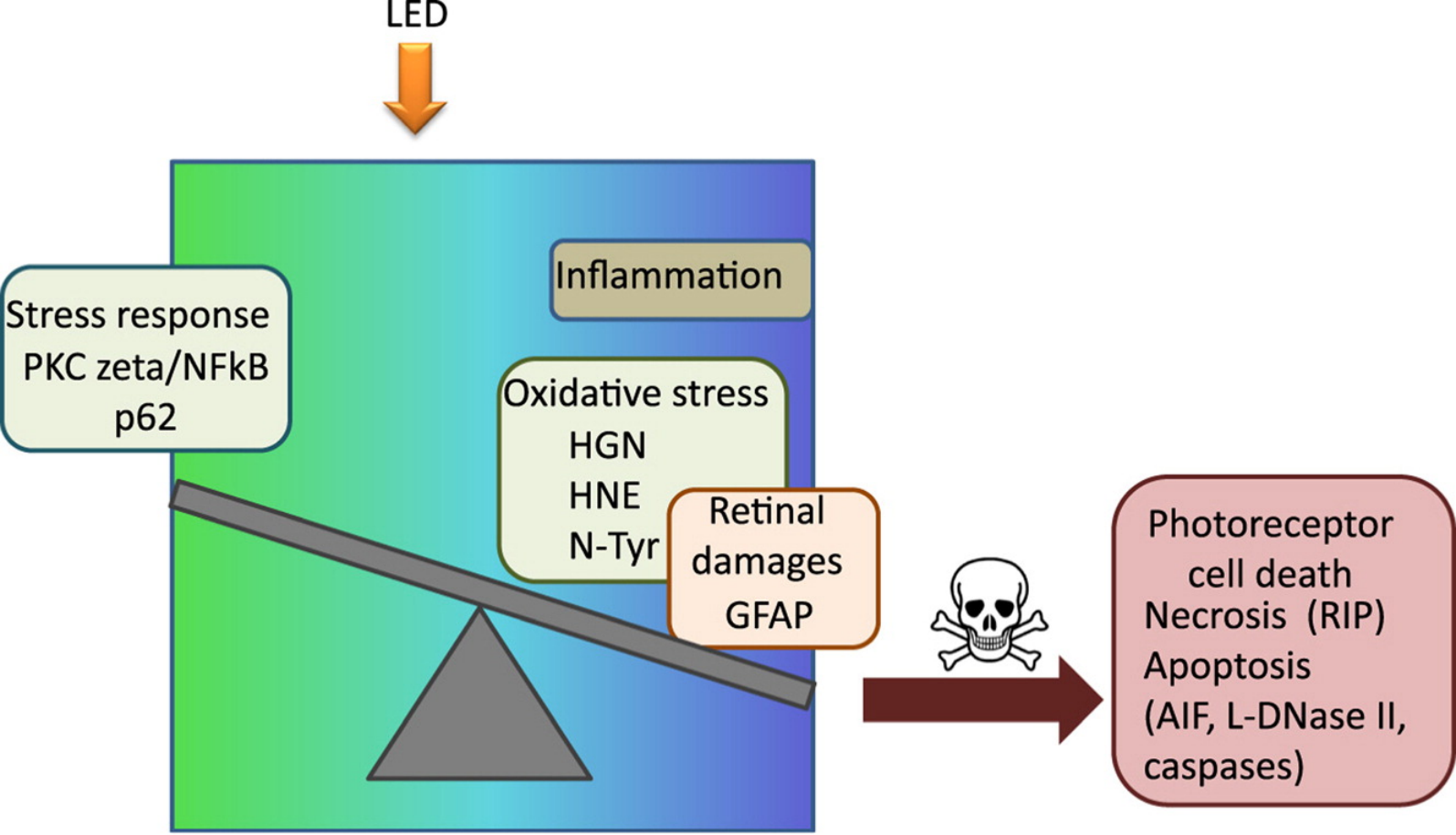

LED have an unbalanced spectrum, rich in blue light.
This is one of the main causes of retinal damage.

Supplementary Information 1

February 20, 2015

1 Dosimetry in the RetinaLED experiment

The dosimetry in the RetinaLED experiment relied on spectrophotometric measurements within the cages and on a model of the Wistar rat vision and behavior.

1.1 Spectrophotometric measurements

For each type of source, the spectral irradiance and spectral irradiance uniformity[1] were measured using a fiber optic spectrophotometer with a diffusing head[2].

The spectral irradiance uniformity in the cage is given by the ratio: $\frac{E_{\lambda,\text{min}}}{E_{\lambda,\text{average}}}$, and was about 0.7 for all cages.

These data were used as parameters to the following model of the Wistar rat retinal illumination.

1.2 Model of the rat retinal irradiance

At a given instant, the corneal spectral irradiance of a (freely moving) rat was dependent upon his head glaze. For the overall dose estimation, it was estimated that on average, a rat keeps his head aligned with his body. In the experiment, only the ceiling of the cage was emitting light. As a consequence, the average corneal spectral irradiance was half the horizontal spectral irradiance, that is: $E_{\lambda,c} = \frac{1}{2} E_{\lambda}$.

Following the arguments given in the review article [1], the retinal irradiance was obtained as the product of the corneal irradiance times the transmittance of the ocular media times the ratio of corneal and retinal illuminated surfaces:

$$E_{\lambda,r} = \tau \, E_{\lambda,c} \, \frac{A_c}{A_r} \qquad [W \cdot m^{-2} \cdot nm^{-1}] \tag{1}$$

where τ is the transmittance of the occular media.

[1] lighting simulations were performed to design the cages such as to maximize the spectral irradiance uniformity.

[2] Ocean Optics HR2000+

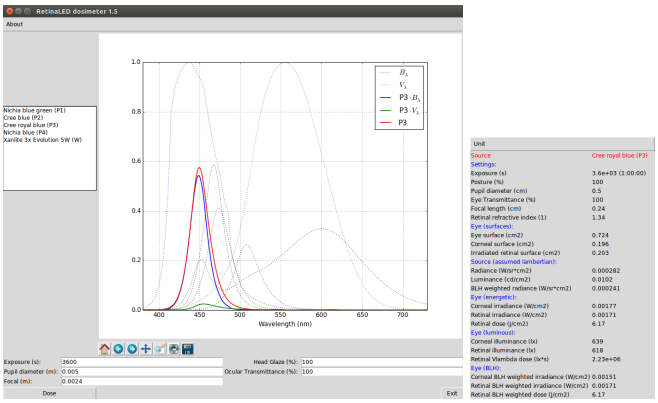

Figure 1: Dedicated dosimetry software (Python language [2]).

The eye of the rat was modeled as a sphere [1]. The area of the cornea was estimated as: $A_c = \frac{\pi d_p^2}{4}$, where d_p is the diameter of the pupil. The area of the illuminated retina was estimated as half that of the ocular globe, *i.e.* $A_r = 2\pi f^2$, where f is the focal length (or equivalently, the diameter of the ocular globe for the emmetropic eye). Thus:

$$E_{\lambda,r} = \tau\, E_{\lambda,c}\, \frac{d_p^2}{8f^2} \qquad [W \cdot m^{-2} \cdot nm^{-1}] \tag{2}$$

The values where $d_p = 5$mm, $f = 2.4$mm and $\tau = 1$.

The irradiance was computed from the spectral irradiance using the relation:

$$E_r = \sum_{\lambda} \Delta_\lambda\, E_{\lambda,r} \qquad [W \cdot m^{-2}] \tag{3}$$

Finally, the retinal dose was computed from the retinal irradiance with:

$$D_r = t\, E_r \qquad [J \cdot m^{-2}] \tag{4}$$

where t is the exposure time.

These dosimetric equations were programmed in a dedicated softwarein order to provide the complete set of illumination parameters during each exposure experiment.

It is noteworthy to mention that although some uncertainities remain in the absolute dose, due to approximation in the head glaze notably, the relative doses between the different sources remain correct.

2 Literature comparison

In the paper, a choice was made to adopt the approach of [1] for the theoretical aspects of the dosimetry. It is noteworthy to mention that other approaches

have been found in the litterature, which are briefly presented here. In any case, although the exact dose received might be different using one method or another, the relative doses remain correct.

In [3], the authors only measure the average irradiance within the cage and its variation during the experiment.

In [4], the eyes of (immobile) rhesus monkeys were exposed using a LASER. The dosimetry was performed as follows. First, the maximum irradiance on the cornea $E_{c,m}$ was estimated based on the Gaussian distribution of the beam:

$$E_r = E_{c,m}\, e^{\frac{-r^2}{2\sigma^2}} \qquad [W \cdot m^{-2}] \tag{5}$$

where E_r is the irradiance at a distance r from the Gaussian peak and σ is calculated from the beam profile by measuring r at $\frac{1}{e^2}$ points. Then, the maximum irradiance on the retina $E_{r,m}$ was estimated from this corneal maximum using:

$$E_{r,m} = \frac{P\tau}{2\pi\sigma^2} \qquad [W \cdot m^{-2}] \tag{6}$$

where P is the power (in watts) entering the cornea and τ is the transmittance of the (rhesus monkey) ocular media.

In [5], another relation was proposed:

$$E_r = \left(\frac{n_2}{n_1}\right)^2 L_c\, \Omega \qquad [W \cdot m^{-2}] \tag{7}$$

where L_c is the incident radiance on the cornea within the solid angle Ω, n_1 is the refractive index of air, n_2 is the refractive index of the ocular media.

References

[1] D. van Norren and T. G. M. F. Gorgels, "The action spectrum of photochemical damage to the retina: a review of monochromatic threshold data.," *Photochem Photobiol*, vol. 87, no. 4, pp. 747–753, 2011.

[2] G. van Rossum, "Python tutorial," Tech. Rep. CS-R9526, Centrum voor Wiskunde en Informatica (CWI), Amsterdam, May 1995.

[3] J. Wu, S. Seregard, B. Spångberg, M. Oskarsson, and E. Chen, "Blue light induced apoptosis in rat retina.," *Eye (Lond)*, vol. 13 (Pt 4), pp. 577–583, Aug 1999.

[4] W. T. Ham Jr, H. A. Mueller, and D. H. Sliney, "Retinal sensitivity to damage from short wavelength light," *Letters to Nature*, vol. 260, pp. 153 – 155, Mar. 1976.

[5] C. Campbell, "Calculation method for retinal irradiance from extended sources.," *Ophthalmic Physiol Opt*, vol. 14, pp. 326–329, Jul 1994.

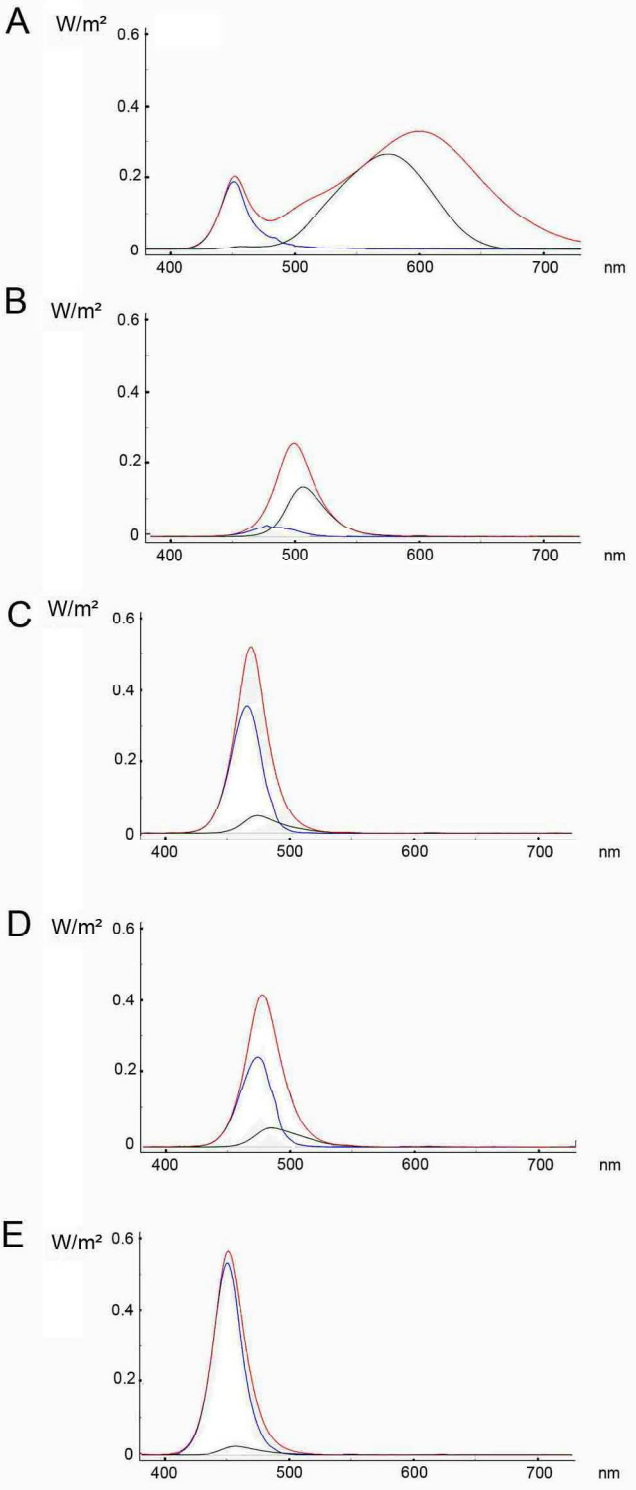
A
W/m²
0.6
0.4
0.2
0
400
500
600
700
nm
B
W/m²
0.6
0.4
0.2
0
400
500
600
700
nm
C
W/m²
0.6
0.4
0.2
0
400
500
600
700
nm
D
W/m²
0.6
0.4
0.2
0
400
500
600
700
nm
E
W/m²
0.6
0.4
0.2
0
400
500
600
700
nm

Figure 1S

A

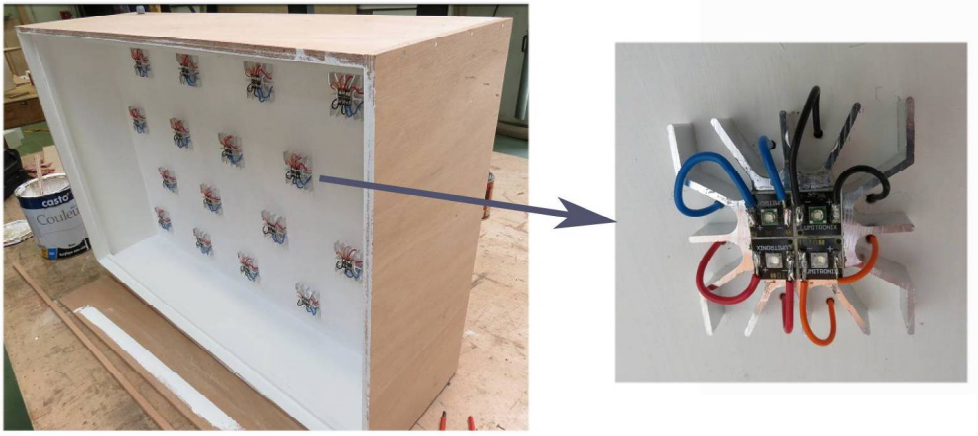

B

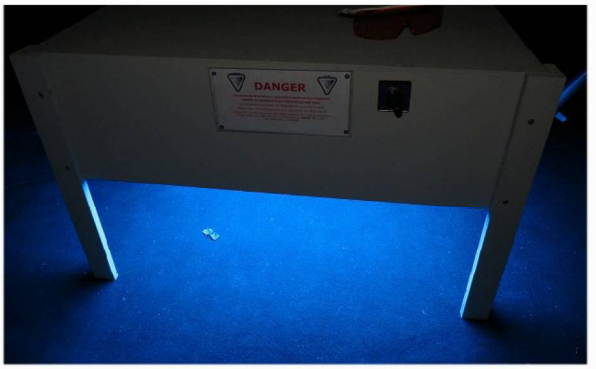

Figure 2S

A

B

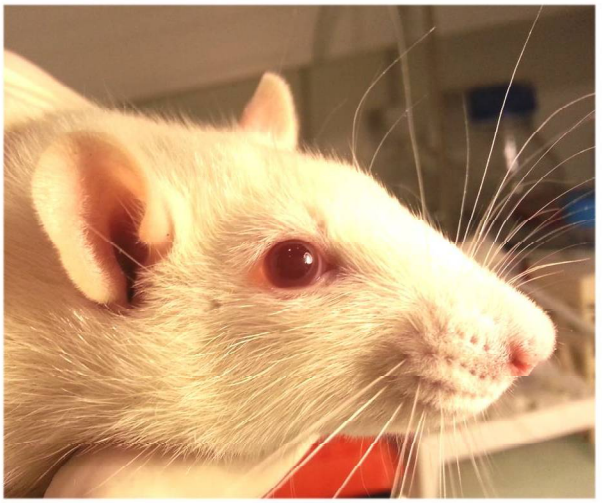

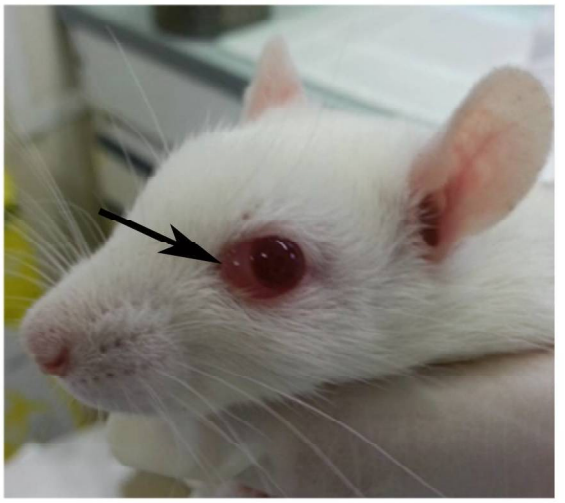

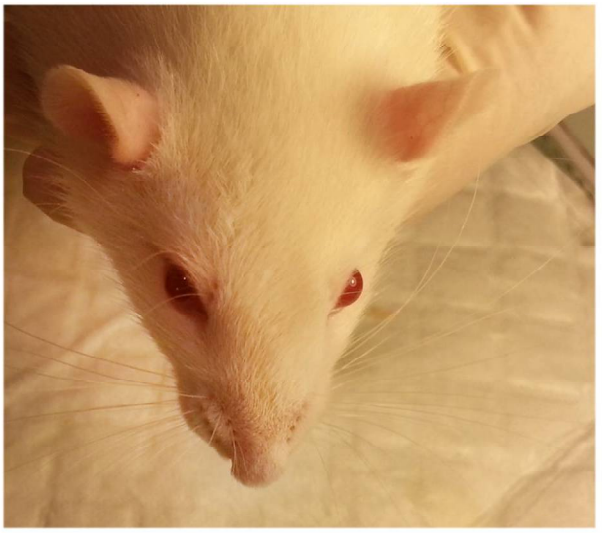

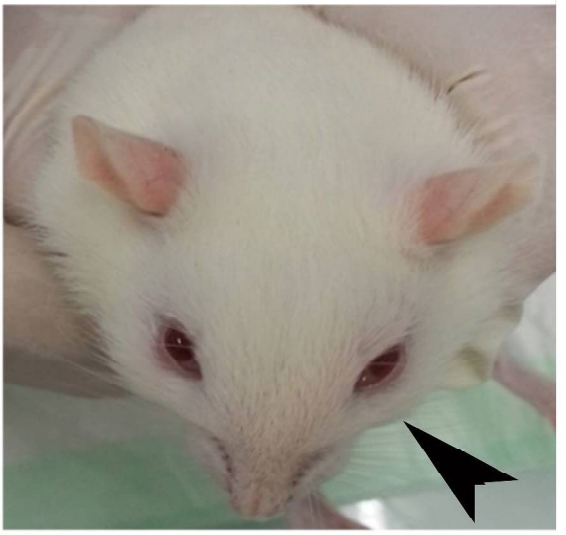

Figure 3 S

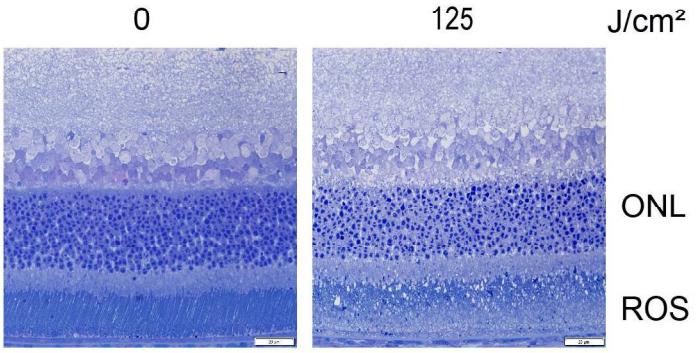

ROS: Rod Outer Segments
ONL: Outer Nuclear Layer

Figure 4S

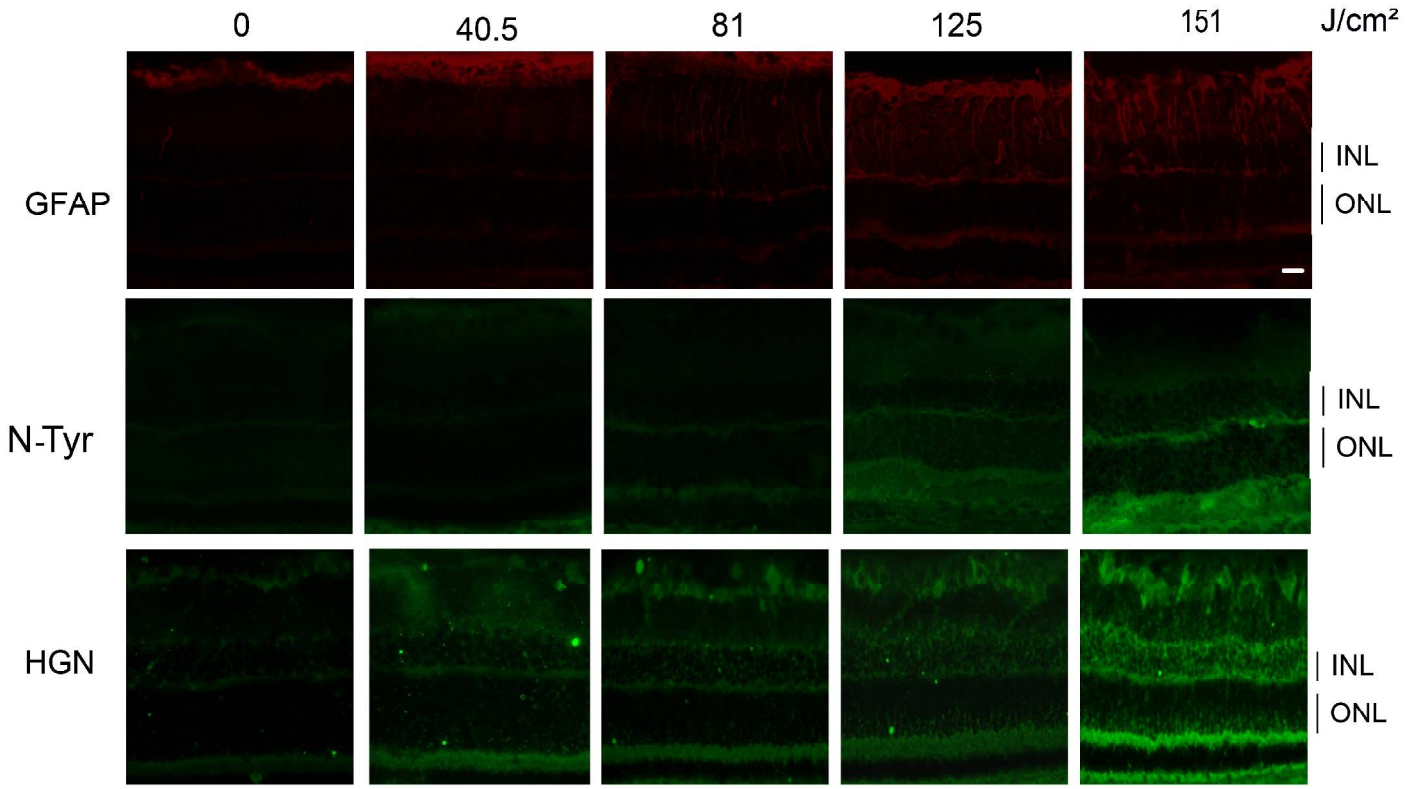

Fig 5S

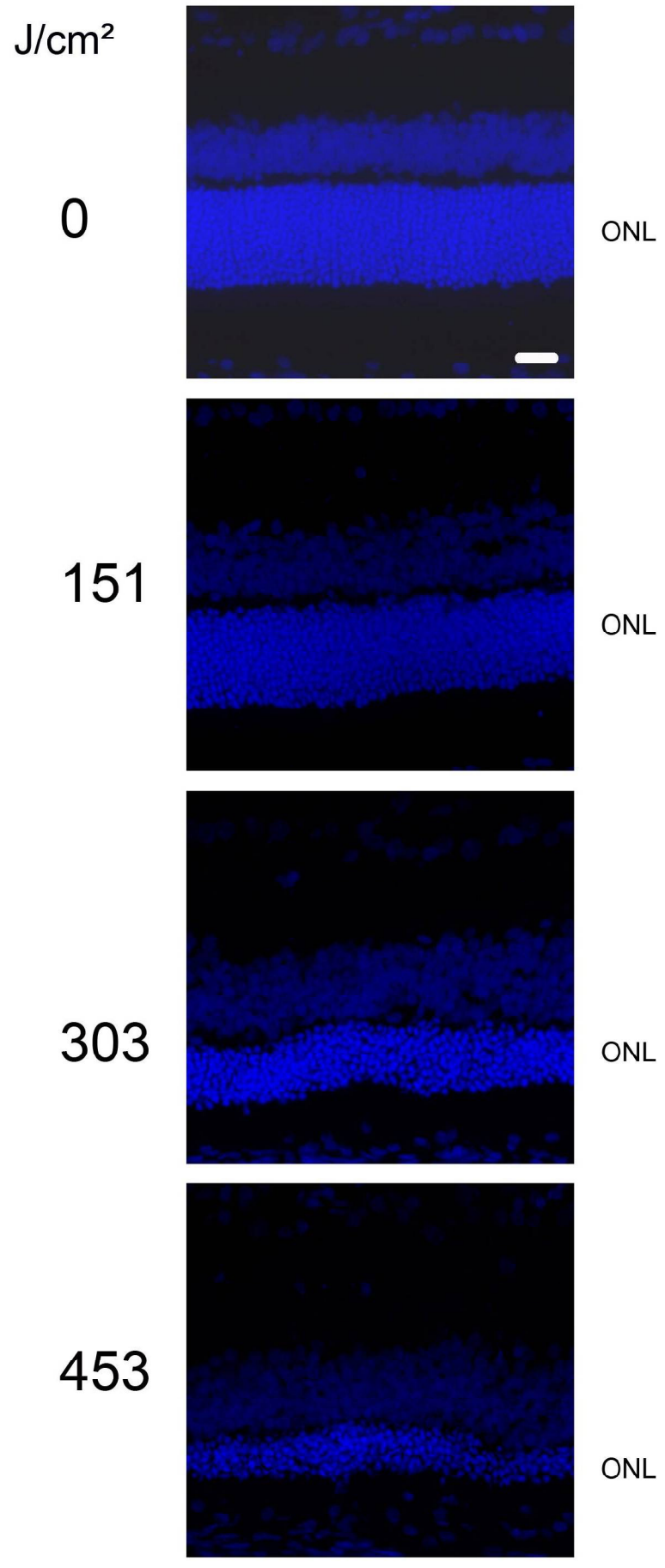

Figure 6S

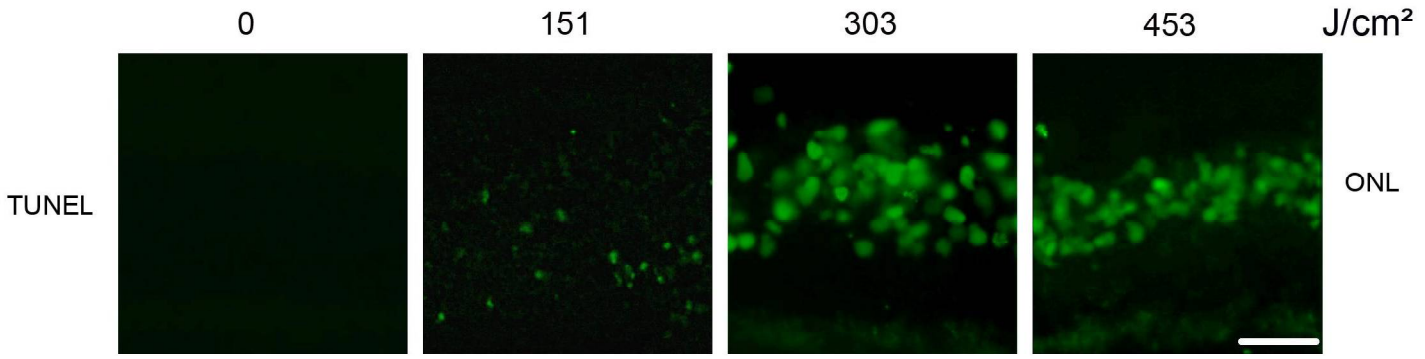

Fig. 7S

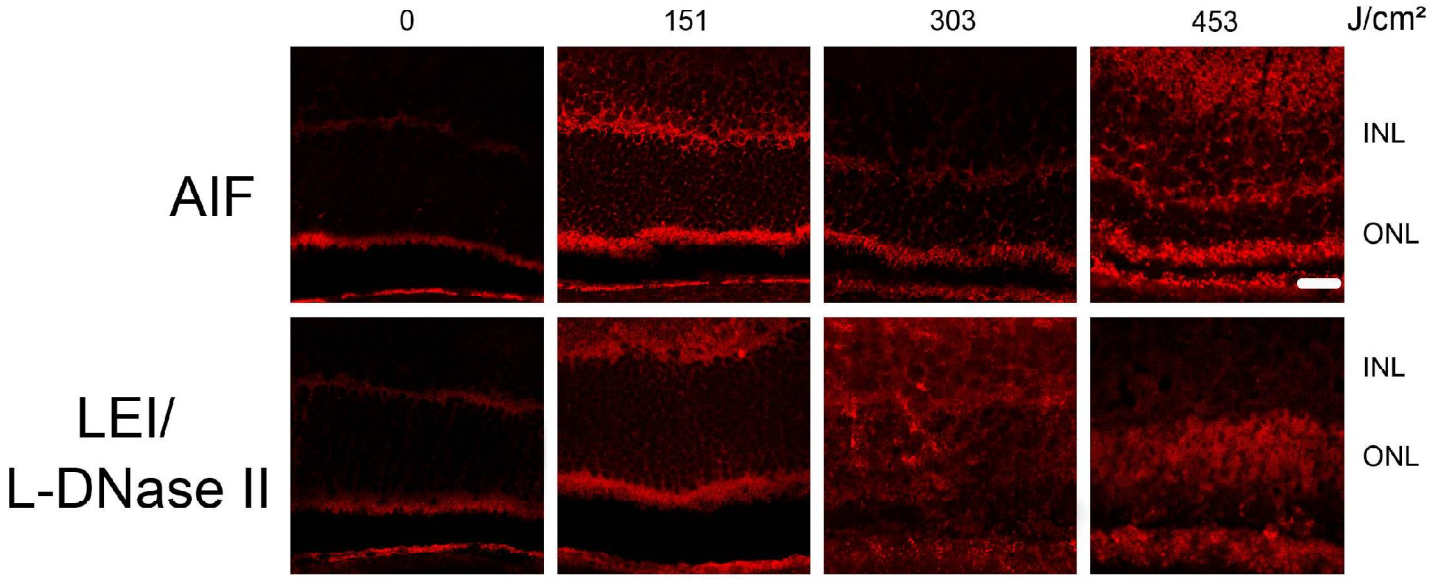

Figure 8S

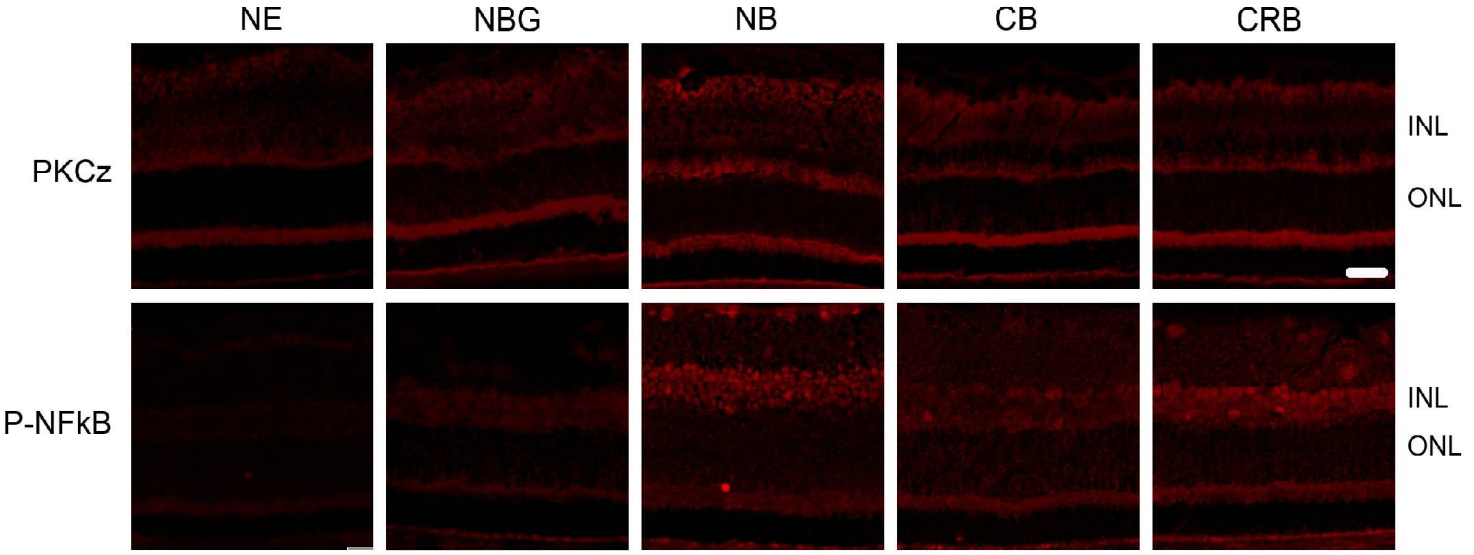

Figure 9S